

Balancing New Against Old Information: The Role of Surprise

Mohammad Javad Faraji,^{1*} Kerstin Preuschoff,^{2#} Wulfram Gerstner^{1#}

¹École Polytechnique Fédérale de Lausanne (EPFL), CH-1015 Lausanne

²University of Geneva, CH-1211 Geneva

*E-mail: mohammadjavad.faraji@epfl.ch

#Co-senior author

Surprise is a ubiquitous concept describing a wide range of phenomena from unexpected events to behavioral responses. We propose a measure of surprise, to arrive at a new framework for surprise-driven learning. There are two components to this framework: (i) a confidence-adjusted surprise measure to capture environmental statistics as well as subjective beliefs, (ii) a surprise-minimization learning rule, or SMiLe-rule, which dynamically adjusts the balance between new and old information without making prior assumptions about the temporal statistics in the environment. We apply our framework to a dynamic decision making task and a maze exploration task to demonstrate that it is suitable for learning in complex environments, even if the environment undergoes gradual or sudden changes. Our proposed surprise-modulated belief update algorithm provides a framework to study the behavior of humans and animals encountering surprising events.

1 Introduction

Humans and animals rely on previously learned knowledge to guide their behavior. A crucial challenge when collecting new data in uncertain environments is the balance between new and old information. How much should we trust what we have learned in the past and how much should we adjust our model of the world based on newly acquired data? In noisy environments, individual data samples are not reliable and a model needs to average over the past data. However, when a structural change occurs in the environment the most recent data samples are the most informative ones and we would want to quickly forget what was learned in the past.

Both humans and animals adaptively adjust the relative contribution of old and newly acquired data on learning (1–4) and rapidly adapt to changing environments (4–6). To capture this behaviour existing models detect and respond to sudden changes using (absolute) reward prediction errors (4, 7), risk prediction errors (8, 9), uncertainty-based jump detection (10, 11) and hierarchical modelling (1, 12). The nature of the environmental change determines which of these models works best. Here we aim to generalize these approaches by using surprise as a trigger for shifting the balance between old and new information.

The Webster dictionary defines surprise as “an unexpected event, piece of information” and “the feeling caused by something that is unexpected or unusual” [merriam-webster.com]. Therefore, surprise is *unexpectedness* and represents the gap between what happens and what was expected to happen.

Behaviorally, surprise can be identified through startle responses (13), which are vital for humans and animals. It manifests itself as physiological responses such as pupil dilation (2, 14) and tenseness in the muscles (13), and can trigger fight-or-flight responses (15).

Neurally, the P300 component of event-related potential (16, 17) measured by electroencephalography is associated with violation of expectation (18, 19). Surprising events have been

shown to influence the development of the sensory cortex (20), and to drive attention (21), as well as learning and memory formation (22–24).

Quantities correlated to surprise have been previously used in machine learning. Planning to be surprised so as to maximize information gain has been suggested as an optimal exploration technique in dynamic environments (25, 26). Signatures of surprise have been observed in artificial models of curiosity and interestingness both of which drive active exploration for learning unknown environments, in the absence of external reward (27). Furthermore, a surprise measure defined as a prediction error has been optimized in the context of free energy minimization (28).

Surprise is difficult to quantify (21, 29–32). Inspired by information theoretic approaches we first introduce a measure of surprise to incorporate subjectivity and uncertainty, two conceptually different aspects of surprise. We formulate the principle of surprise minimization as a learning strategy and derive a class of learning rules which obey that principle. We then propose a *surprise-modulated* belief update rule that can be used for learning within changing environments. We apply our proposed method to a dynamic decision making task in a Gaussian environment, as well as an exploration task in a maze-like environment. We demonstrate how surprise and uncertainty interact with each other to make learning in changing environments possible. Finally, we discuss implications of surprise in reinforcement learning and link surprise and its role in learning/plasticity to existing neurophysiological evidence and behavioral data.

2 Theory

Surprise occurs whenever there is *uncertainty*, be it in the world or in the model that we build of the world. While the former corresponds to the probabilistic nature of the world, the latter is caused by an imperfect internal model of the outside world.

We emphasize that surprise is *subjective*: events that are surprising to me may not be surprising to you, although we may both have used the same data to build our models of the world. Subjectivity may arise from different methods for building our internal models, or different prior beliefs about the world (29, 30). Model uncertainty differs from subjectivity in that the former refers to uncertainty in parameter estimation given the available data that remains even in the "best" model (e.g., Bayes-optimal). The latter incorporates individual differences in the construction of a (potentially suboptimal) model given identical data.

In order to quantify surprise, we assume that the world is governed by a set of parameters θ^* chosen by nature. If θ^* is known, the *information content* $-\ln p(X|\theta^*)$ for a specific outcome $X \in \mathcal{X}$ is a measure of surprise (30–32) which says that the occurrence of a rare (i.e., unlikely to occur) data sample X is surprising. As the information content relates to the *true* probabilities $p(X|\theta^*)$ of samples in the *real* world, it is an *objective*, model-independent, measure of unexpectedness. However, the true set of parameters θ^* , and so the true probability $p(X|\theta^*)$, is rarely known to the observer, such that it is difficult to evaluate the exact information content of a data sample X .

The Bayesian framework bypasses this issue by modeling the world as a joint distribution $p(X, \theta) = p(X|\theta)\pi_0(\theta)$ which specifies how data X is generated if the model parameter is $\theta \in \Theta$. The prior distribution $\pi_0(\theta)$ represents the current belief of the observer about the likelihood of the world having parameters θ . We define the *raw* surprise $S_{raw}(X; \pi_0)$ of a data sample X as

$$S_{raw}(X; \pi_0) := - \int_{\Theta} \pi_0(\theta) \ln p(X|\theta) d\theta, \quad (1)$$

where we replaced the exact information content with a weighted average over all possible model parameters. In contrast to the information content, the raw surprise (1) is a *subjective*, model-dependent, measure of unexpectedness. Therefore, the same data point X might differently surprise different people, as they may have different beliefs $\pi_0(\theta)$ about model parameters.

2.1 Confidence-corrected surprise

In addition to the raw surprise (1) being subjective we would also like to capture the impact of a subject's *confidence* in her belief. Intuitively, if we are uncertain about what to expect (because we have not yet learned the structure of the world), receiving a data sample that occurs with low probability under the present model is less surprising than a low-probability sample in a situation when we are almost certain about the world (see Fig.1A). Our confidence about the current model of the world is represented by the *entropy* $\mathcal{H}(\pi_0) = - \int_{\Theta} \pi_0(\theta) \ln \pi_0(\theta) d\theta$ of our current belief about the model parameters. To arrive at the *confidence-corrected surprise*, we first subtract the entropy $\mathcal{H}(\pi_0)$ of our current belief from the raw surprise, i.e.,

$$S_{raw}(X; \pi_0) - \mathcal{H}(\pi_0) = \int_{\Theta} \pi_0(\theta) \ln \frac{\pi_0(\theta)}{p(X|\theta)} d\theta. \quad (2)$$

While the right-hand side of equation (2) is reminiscent of a KL divergence (between $\pi_0(\theta)$ and $p(X|\theta)$ as a function of θ), the likelihood function $p(X|\theta)$ is *not* a correctly normalized probability distribution function with respect to θ . To rewrite equation (2) as a KL divergence, we divide the likelihood $p(X|\theta)$ by a scaling factor $\|p_X\| = \int_{\Theta} p(X|\theta') d\theta'$. The *scaled likelihood* $\hat{p}_X(\theta) = \frac{p(X|\theta)}{\|p_X\|}$ can be considered as a probability distribution function over θ , just like the prior $\pi_0(\theta)$. The normalization corresponds to calculating the posterior under a *flat* prior (see Appendix A). The divergence $D_{KL}[\pi_0(\theta) \|\hat{p}_X(\theta)]$ is a well-defined quantity, which we use to define the confidence-corrected surprise

$$S_{corr}(X; \pi_0) = D_{KL}[\pi_0(\theta) \|\hat{p}_X(\theta)] = \int_{\Theta} \pi_0(\theta) \ln \frac{\pi_0(\theta)}{\hat{p}_X(\theta)} d\theta. \quad (3)$$

The confidence-corrected surprise measure (3) represents the difference between what we expected to happen (as indicated by the current belief $\pi_0(\theta)$) and what actually happened in the world: the relevance of a new data point X is indicated by the (scaled) likelihood $\hat{p}_X(\theta)$. As such we have defined a surprise measure that meets our requirements: a subjective, confidence-

adjusted measure of the difference between expectation and realization. We emphasize that the confidence-corrected surprise is evaluated for each data point X separately.

2.2 Surprise minimization: the SMiLe-rule

Successful learning implies an adaptation to the environment such that an event occurring for a second time is perceived as less surprising than the first time. In the following *surprise minimization* refers to a learning strategy which modifies the internal model of the external world such that the unexpected observation becomes less surprising if it happens again in the near future. Surprise minimization is akin to - though more general than - reward prediction error learning. Reward based learning modifies the reward expectation such that a recurring reward results in a smaller reward prediction error. Similarly, surprise-minimization learning results in a smaller surprise for recurring events.

To mathematically formulate learning through surprise minimization, we define a *learning rule* $L(X, \pi_0)$ as a mapping from a prior belief $\pi_0(\theta)$ to a posterior belief $q(\theta)$ after receiving data sample X , i.e., $q = L(X, \pi_0)$. Moreover, we define a *belief update* as the learning step after a single data sample.

We define the class \mathcal{L} of *plausible* learning rules as the set of those learning rules L for which the surprise $\mathcal{S}(X; q)$ of *any* data sample X under the posterior belief $q(\theta)$ is *at most as surprising as* the surprise $\mathcal{S}(X; \pi_0)$ of that data sample under the prior belief $\pi_0(\theta)$, i.e.,

$$\mathcal{L} = \{L : \mathcal{S}(X; q) \leq \mathcal{S}(X; \pi_0), q = L(X, \pi_0), \forall X \in \mathcal{X}\}. \quad (4)$$

In other words, if the same data sample X occurs a second time right after a belief update, it is perceived as less surprising than the first time.

After the belief update we can measure how much the new data X has impacted the internal model by comparing the surprise of data sample X under the posterior belief to its surprise

under the prior belief:

$$\Delta\mathcal{S}(X; L) = \mathcal{S}(X; \pi_0) - \mathcal{S}(X; q). \quad (5)$$

Given a learning rule L , a data sample X is considered more effective for a belief update than X' , if $\Delta\mathcal{S}(X; L) > \Delta\mathcal{S}(X'; L)$. Note that definitions (4, 5) do not depend on our specific choice of surprise measure \mathcal{S} . In the following we choose \mathcal{S} to be the confidence-corrected surprise S_{corr} (3).

The *impact function* $\Delta S_{corr}(X; L)$ (5), for a given data sample X , is maximized by the learning rule that maps the prior belief $\pi_0(\theta)$ to the scaled likelihood $\hat{p}_X(\theta)$. However, as this posterior distribution $q = \hat{p}_X$ does not depend on the prior belief π_0 , it discards all previously learned information. Therefore, it amounts to a valid though meaningless solution.

To avoid overfitting to the last data sample, we need to limit our search to posteriors q that are not too different from the prior π_0 . This limited set can be expressed as the set of posteriors q that fulfill the constraint $D_{KL}[q||\pi_0] \leq B$, for some non-negative upper bound $B \geq 0$. The parameter B determines how much we allow our belief to change after receiving a data sample X . Maximizing the impact function $\Delta S_{corr}(X; L)$ under such a constraint, is equivalent to the following constraint optimization problem:

$$\min_{q: D_{KL}[q||\pi_0] \leq B} S_{corr}(X; q). \quad (6)$$

Using the method of Lagrange multipliers we find the solution of problem (6) to be

$$q_\gamma(\theta) = \frac{p(X|\theta)^\gamma \pi_0(\theta)^{1-\gamma}}{Z(X; \gamma)}, \quad (7)$$

where $Z(X; \gamma) = \int_{\Theta} p(X|\theta)^\gamma \pi_0(\theta)^{1-\gamma} d\theta$ is a normalizing factor and $0 \leq \gamma \leq 1$ is uniquely determined by the bound B (see Appendix **B** for the proof). The unique relationship between γ and B means that once B has been chosen, γ is no longer a free parameter and vice versa.

We call the learning rule (7) *surprise minimization learning (SMiLe)*. It is reminiscent of Bayes' rule except for the parameter γ which modulates the relative contribution of the

likelihood $p(X|\theta)$ and the prior $\pi_0(\theta)$ to the posterior $q(\theta)$. Note that the SMiLe rule belongs to the class \mathcal{L} of plausible learning rules, for all $0 \leq \gamma \leq 1$.

Choosing γ in the range $0 \leq \gamma \leq 1$ is equivalent to choosing a bound $B \geq 0$. To understand how the optimal solution (7) - and thus γ - relates to the boundary B , we illustrate its limiting cases (see Fig. 1B): (i) $B = 0$ yields $\gamma = 0$ and the posterior q is identical to the prior π_0 . In other words, the new information is discarded. (ii) For $B \geq B_{max} = D_{KL}[\hat{p}_X||\pi_0]$, the solution is always the scaled likelihood \hat{p}_X (corresponding to $\gamma = 1$) because $q = \hat{p}_X$ fulfills the constraint $D_{KL}[q||\pi_0] \leq B$ for any $B \geq B_{max}$ and minimizes $S_{corr}(X; q)$ among all posteriors q . This is equivalent to the unconstrained case, and implies that all previous information is discarded. (iii) For $0 < B < B_{max}$ the optimal solution is the posterior q_γ , Eq. (7), with $0 < \gamma < 1$ satisfying $D_{KL}[q_\gamma||\pi_0] = B$. Moreover, $B > B'$ implies $\gamma > \gamma'$ (see Fig. 1B).

While the SMiLe rule (7) depends on a parameter γ which is uniquely determined by the bound B we have yet to indicate how to choose B . Highly surprising data should result in larger belief shifts. As such, the bound B should increase with the level of surprise. We choose a simple monotonic function to link the bound to the surprise. In the following, for each data sample X , we take

$$B(X) = \frac{m S_{corr}(X; \pi_0)}{1 + m S_{corr}(X; \pi_0)} B_{max}(X), \quad (8)$$

where $B_{max}(X) = D_{KL}[\hat{p}_X||\pi_0]$. Here, the monotonic function depends on a subject-specific parameter m that describes an organism's propensity toward changing its belief. Note that in Eq. (8) $m = 0$ indicates that the subject will never change her belief. As m increases so does a subject's willingness to change her belief. Thus, differences in m from one subject to the next will eventually allow us to capture heterogeneity in belief update strategies.

The exact link between the bound and surprise is not crucial as long as B is monotonic in surprise in a *reasonable* way. Note that biological correlates of surprise such as pupil dilation or the activity of a neuromodulator will normally saturate at some maximal value - consistent

with our choice of a saturating function in Eq. (8).

2.3 Surprise-modulated belief update

The surprise-modulated belief update combines the confidence corrected surprise (3) and the SMiLe rule (7) to dynamically update our belief: after receiving a new data point X , we evaluate the surprise $S_{corr}(X; \pi_0)$ which sets the bound for our update and allows us to solve for γ . We then update the belief, using the SMiLe rule (7) with parameter γ (see Algorithm 1).

Algorithm 1 Pseudo algorithm for surprise-modulated belief update (SMiLe)

- 1: $N \leftarrow$ number of data samples
- 2: Belief $\leftarrow \pi_0$ (the prior belief)
- 3: $m \leftarrow 0.1$ (subject-dependent)
- 4: **for** n : 1 to N **do**
- 5: $X_n \leftarrow$ a new data sample
- 6: (i) evaluate the surprise $S_{corr}(X_n; \text{Belief})$, Eq. (3)
- 7: (ii-a) calculate $B_{max}(X_n) = D_{KL}[\hat{p}_{X_n} || \text{Belief}]$
- 8: (ii-b) choose the bound $B(X_n) = \frac{m S_{corr}(X_n; \text{Belief})}{1 + m S_{corr}(X_n; \text{Belief})} B_{max}(X_n)$
- 9: (iii) find γ by solving $D_{KL}[q_\gamma || \text{Belief}] = B(X_n)$
- 10: (iv) update using SMiLe, Eq. (7): $\text{Belief}(\theta) \leftarrow \frac{p(X_n|\theta)^\gamma \text{Belief}(\theta)^{1-\gamma}}{\int_{\Theta} p(X_n|\theta)^\gamma \text{Belief}(\theta)^{1-\gamma} d\theta}$
- 11: **Return** Belief;

Note 1: In each iteration, we first calculate the surprise, step (i), before the model is updated in step (iv).

Note 2: The steps (ii-a), (ii-b), and (iii) can be merged and approximated by $\gamma = f(S_{corr}(X_n; \text{Belief}))$ where $f(\cdot)$ is a subjective function that increases with surprise.

The parameter γ in the SMiLe rule (7) controls the *impact* of a data sample X on belief update such that a bigger γ causes a larger impact. More precisely, the impact function $\Delta S_{corr}(X, L)$ (5), where L is replaced by the SMiLe rule (7), is an increasing function of γ (see Appendix C for the proof).

We note that in classical models of perception and attention (21, 29), surprise has been defined as a measure of belief change (such as $D_{KL}[q_\gamma || \pi_0]$ or its mirror form $D_{KL}[\pi_0 || q_\gamma]$). We

emphasize that our model of surprise is "fast" in the sense that it can be evaluated *before* the beliefs are changed. Interestingly, the impact function is linked to the measures of *belief change* by the following equation (see Appendix **D** for derivation),

$$\Delta S_{corr}(X, L) = \frac{1}{\gamma} D_{KL}[\pi_0 || q_\gamma] + \left(\frac{1}{\gamma} - 1\right) D_{KL}[q_\gamma || \pi_0] \geq 0. \quad (9)$$

Therefore *a larger reduction in the surprise implies a bigger change in belief.*

3 Simulations

In the following we will look at two examples to illustrate the functionality of our proposed surprise-modulated belief update algorithm 1. The first is a simple, one-dimensional, dynamic decision making task which has been used in behavioral studies (1, 2) of learning under uncertainty. While somewhat artificial as a task, it is appealing as it nicely isolates different forms of uncertainty. This allows us to (i) demonstrate the basic quantities and properties of our algorithm and (ii) show how its flexibility allows it to capture a wide range of behaviours. The second example is a multi-dimensional maze-exploration task which we will use to demonstrate how our algorithm extends to and performs in more complex and realistic experimental environments.

3.1 Gaussian estimation

Task. In the one-dimensional dynamic decision making task subjects are asked to estimate the mean of a distribution based on consecutively and independently drawn samples. At each time step n , a data sample X_n is drawn from a normal distribution $\mathcal{N}(\mu_n, \sigma_x^2)$ and the subject is asked to provide her current estimate $\hat{\mu}_n$ of the mean of the distribution. Throughout the experiment, the mean may change without warning (Fig. 2A). Changes occur with a hazard rate 0.066. The variance σ_x^2 remains fixed.

Model. We model the subject’s belief *before* the n -th sample X_n is observed, as the normal distribution $\mathcal{N}(\hat{\mu}_{n-1}, \sigma_{n-1}^2)$ where $\hat{\mu}_{n-1}$ is the estimated mean and σ_{n-1}^2 determines how uncertain the subject is about her estimation. In order to keep the scenario as simple as possible, we assume $\sigma_0^2 = \sigma_x^2$. The posterior mean $\hat{\mu}_n$ resulting from the surprise-modulated belief update (algorithm 1) is a *weighted average* of the prior mean $\hat{\mu}_{n-1}$ and the new sample X_n (see Appendix E for derivation),

$$\hat{\mu}_n = \gamma X_n + (1 - \gamma)\hat{\mu}_{n-1}. \quad (10)$$

The weight factor, that determines to what extent a new sample X_n affects the posterior mean $\hat{\mu}_n$, is determined by γ which increases with the surprise $S_{corr}(X_n)$ of that sample (Fig. 2B), i.e.,

$$\gamma = \sqrt{\frac{mS_{corr}(X_n)}{1 + mS_{corr}(X_n)}}, \quad S_{corr}(X_n) = \frac{(X_n - \hat{\mu}_{n-1})^2}{2\sigma_x^2}. \quad (11)$$

Note that in this example, the confidence-corrected surprise measure is related to the *normalized unsigned prediction error* $|X_n - \hat{\mu}_{n-1}|/\sigma_x$. This outcome of our SMiLe-update is consistent with recent approaches in reward learning that suggest to use reward prediction errors scaled by standard deviation or variance (8).

Results. The confidence-corrected surprise increases suddenly in response to the samples immediately after the change points, as they are unexpected under the current prior. As a consequence, surprising samples increase the influence of a new data sample on the posterior mean (Fig. 2B). We can compare our surprise modulated belief update in Eqs. (10), (11) with a delta-rule (10) with *constant* weighting factor γ . To enable a fair comparison we consider two situations: (i) we arbitrarily fix γ at 0.5 or (ii) for a given *hazard rate* H we first search for the optimal value of fixed γ so as to minimize the estimation error (Fig. 2C). We find that our surprise-modulated belief update outperforms the delta-rule with *any* constant learning rate (Fig. 2D). This clearly shows that an adaptive learning rate is preferable to a fixed learning rate.

We also compared our proposed algorithm with a delta-rule that approximates the optimal Bayesian solution (10). In the optimal model the subjects knows a-priori that the mean will change at unknown points in time, leading to a hierarchical statistical model of the world. The algorithm proposed in (10) provides an efficient approximate algorithm to estimate the parameters of the hierarchical model. In this algorithm, the subject increases the learning rate as a function of probability of encountering a change point at a given time step. This probability requires knowledge or online estimation of the hazard rate, which indicates how frequently change points occur. Although our surprise-modulated belief update does not outperform the approximate Bayesian delta-rule, the difference in performance is, in most cases, not significant (see Fig. 2D). In other words, our method, which does not require any information about the hazard rate, can approximate the quality of the optimal Bayesian solution, with significantly reduced computational complexity.

3.2 Maze exploration

Task. The maze exploration task is similar to tasks used in behavioral neuroscience and robotics (33–35). There are two environments \mathcal{A} and \mathcal{B} each composed of the same uniquely labeled (e.g., by colors or cue cards) rooms. \mathcal{A} and \mathcal{B} only differ in the topology / spatial arrangement of rooms (see Fig. 3). Neighboring rooms are connected and accessible through doors. Initially, the agent is placed into either \mathcal{A} or \mathcal{B} . At each time step a door of the current room opens and the agent moves into the adjacent room, thus exploring the environment. After a random exploration time the environment is switched. Once it is changed, the agent must quickly adapt to the new environment. Note that this task differs from a reinforcement learning task because the task at hand just consists of the *exploration* phase. In particular, there is no reward involved in learning.

Model. We model the knowledge of the environment by a learning agent that updates a

set of parameters $\alpha(s, \check{s}) \geq 1$ used for describing its belief about *state transitions* from $s \in \{1, 2, \dots, 16\}$ to $\check{s} \in \{1, 2, \dots, 16\} \setminus s$, where 16 is the number of rooms. More precisely, an agent’s belief about how likely it is to visit \check{s} , given the current state s , is modeled by a *Dirichlet distribution* parametrized by a *vector* of parameters $\vec{\alpha}(s) \in \mathbb{R}^{15}$. The components of the vector $\vec{\alpha}(s)$ are denoted as $\alpha(s, \check{s})$.

The surprise-modulated belief update (algo 1), with the Dirichlet distribution inserted, yields algorithm 2 for the maze exploration task (see Appendix F for derivation). Immediately after a transition from the current state s to the next state s' , the posterior belief q_γ obtained by the SMiLe rule (7) is a Dirichlet distribution $\vec{\alpha}_{new}(s)$ with components $\alpha_{new}(s, \check{s}) = \gamma(1 + [\check{s} = s']) + (1 - \gamma)\alpha_{old}(s, \check{s})$, that can be written as a *weighted average* of the parameters of the prior belief π_0 (i.e., $\alpha_{old}(s, \check{s})$) and those of the scaled likelihood \hat{p}_X (i.e., $1 + [\check{s} = s']$). Here, $[\check{s} = s']$ indicates a number that is 1 if the condition in square brackets is satisfied, and 0 otherwise.

In order to see how well our proposed surprise-modulated belief update algorithm performs in this task, we compare it with a naive Bayesian learner and an online expectation-maximization (EM) algorithm (36). While in the former the agent assumes that there is only a single stable, but stochastic environment, the latter benefits from knowing the true hidden Markov model (HMM) of the task and approximates the optimal hierarchical Bayesian solution (see Appendix G).

Results. Similar to the Gaussian mean estimation task, surprise is initially high and slowly decreases as the agent learns the topology of the environment (Fig. 4A). When the environment is switched, the sudden increase in the surprise signal (Fig. 4A) causes the parameter γ to increase (Fig. 4B). This is equivalent to discounting previously learned information and results in a quick adaptation to the new environment. To quantify the adaptation to the new environment, we compare the state transition probabilities of the current model with the true transition probabilities of the two environments. We find that the estimation error of the state transition

Algorithm 2 Surprise-modulated belief update for the maze exploration task

- 1: $N \leftarrow$ number of data samples
- 2: $\alpha(s, \check{s}) = 1, \quad \forall s \in \{1, 2, \dots, 16\}, \check{s} \in \{1, 2, \dots, 16\} \setminus \{s\}$ (a uniform prior belief)
- 3: $m \leftarrow 0.1$ (subject-dependent)
- 4: Start in state s
- 5: **for** n : 1 to N **do**
 - # at this time step we only update the parameters that describe state transitions from the current state s to all possible next states $\check{s} \in \{1, 2, \dots, 16\} \setminus \{s\}$. The prior belief, for the state s , is $\pi_0 \sim Dir(\mathbf{a}), \mathbf{a} \in \mathbb{R}^{15}, \mathbf{a}(\check{s}) = \alpha(s, \check{s})$.
- 6: $X_n : s \rightarrow s'$ (a new transition is observed)
 - # the scaled likelihood is $\hat{p}_X \sim Dir(\mathbf{b}), \mathbf{b} \in \mathbb{R}^{15}, \mathbf{b}(\check{s}) = 1 + [\check{s} = s']$
- 7: (i) $S_{corr}(X_n; \pi_0) = D_{KL}[Dir(\mathbf{a}) || Dir(\mathbf{b})]$
- 8: (ii-a) $B_{max}(X_n) = D_{KL}[Dir(\mathbf{b}) || Dir(\mathbf{a})]$
- 9: (ii-b) $B(X_n) = \frac{m S_{corr}(X_n; \pi_0)}{1 + m S_{corr}(X_n; \pi_0)} B_{max}(X_n)$
- 10: (iii) find γ by solving $D_{KL}[Dir(\gamma \mathbf{b} + (1 - \gamma) \mathbf{a}) || Dir(\mathbf{a})] = B(X_n)$
- 11: (iv) $\alpha(s, \check{s}) \leftarrow (1 - \gamma) \alpha(s, \check{s}) + \gamma (1 + [\check{s} = s'])$
- 12: **Return** $\alpha(s, \check{s}), \forall s, \check{s}$;

Note 1: $D_{KL}[Dir(\mathbf{m}) || Dir(\mathbf{n})] = \ln \Gamma(\sum_{\check{s}} \mathbf{m}(\check{s})) - \ln \Gamma(\sum_{\check{s}} \mathbf{n}(\check{s})) - \sum_{\check{s}} \ln \Gamma(\mathbf{m}(\check{s})) + \sum_{\check{s}} \ln \Gamma(\mathbf{n}(\check{s})) + \sum_{\check{s}} (\mathbf{m}(\check{s}) - \mathbf{n}(\check{s})) (\Psi(\mathbf{m}(\check{s})) - \Psi(\sum_{\check{s}} \mathbf{m}(\check{s})))$.

Note 2: $\Gamma(\cdot)$ and $\Psi(\cdot)$ denote the *gamma* and *digamma* functions, respectively. $[\check{s} = s']$ denotes the Iverson bracket, a number that is 1 if the condition in square brackets is satisfied, and 0 otherwise.

probabilities in the new environment is quickly reduced after the switch points (Fig. 4C). Following a change point, the model uncertainty, measured as the entropy of the current belief about the state transition probabilities, increases indicating that the current model of the topology is inaccurate (Fig. 4D). A few time steps later the uncertainty slowly decreases, indicating increased confidence in what is learned in the new environment.

If we look more closely at the model parameters, we find that the surprise-modulated belief update (algorithm 2) enables the agent to adjust the estimated state transition probabilities. In Fig. 5 we compare the estimated and the true transition probabilities 100 time steps after a switch. Given that the environment is characterized by 64 different transitions (in a space of $16 \times 15 = 240$ potential transitions), 100 time steps allow an agent to explore only a fraction of the potential transitions. Nevertheless, 100 time steps after a switch the matrix of transition probabilities already resembles that of the present environment (Figs. 5C, 5D).

Surprise-modulated belief update is a method of quick learning. How well does our SMiLe update rule perform to other existing models? We compared it with two well-known models. First, a naive Bayesian learner which tries to estimate the 240 state transition probabilities, by Bayes rule. Note that, by construction, the naive Bayesian learner is not aware of the switches between the environments. Second, a hierarchical statistical model that reflects the architecture of the *true world* as in Fig. 3. The task is to estimate the 2×240 state transitions in the two environments as well as transition probabilities between the environments $p_{A \rightarrow B}$ and $p_{B \rightarrow A}$ by an online EM algorithm.

For the naive Bayesian learner, we find that its behavior indicates a steady increase in certainty, regardless of how surprising the samples are. In other words, it is incapable of changing its belief after it has sufficiently explored the environments (Fig. 4C). The state transition probabilities are estimated by averaging over the true parameters of both environment, where the weight of averaging is determined by the fraction of time spent in the corresponding environ-

ment (Figs. 5E, 5F).

The comparison of our surprise modulated belief update with the online EM algorithm for the hierarchical Bayesian model associated with the switching environments, provides several insights (see Fig. 6). First, already after less than 1000 time steps, the estimation error for environment \mathcal{A} during short episodes in environment \mathcal{A} drops below $E_{\mathcal{A}} = 0.002$. Only after 10000 time steps, the online EM algorithm achieves the same level of accuracy. While the solution of the SMiLe rule in the long run is not as good, our algorithm benefits from a reduced computational complexity and simpler implementation.

To further investigate the ability of an agent to adapt to the new environment after a switch, we analyzed performance as a function of two free parameters that control the setting of the task: (i) the fraction of time spent in environment \mathcal{A} , and (ii) the average time spent in environment \mathcal{A} before a switch to \mathcal{B} occurs. To do so, we calculate the average estimation error in state transition probabilities 64 time steps after a switch occurs. We consider only those switches after which the agent stays in that environment for *at least* 64 time steps. Note that 64 is the minimum number of time steps that is required to make sure that all possible transitions from 16 room to their 4 neighbors *could* occur. A smaller estimation error for a given pair of free parameters indicates a faster adaptation to the new environment for that setting.

We found that the surprise-modulated belief enables an agent to quickly readjust its estimation of model parameters, even if the fraction of time spent in an environment is relatively short. In that sense, it behaves similarly to the approximated hierarchical Bayesian approach (online EM algorithm). This is not, however, the case for a naive Bayesian learner whose estimation error in each environment depends on the fraction of time spent in that corresponding environment (see Fig. 7).

The naive Bayesian learner suffers from low accuracy in estimation and cannot adapt to environmental changes. A full hierarchical Bayesian model, however, requires prior informa-

tion about the task and is computationally demanding. For example, the computational load of the hierarchical Bayesian model increases with the number N of environments between which switching occurs. The surprise-modulated belief update, however, balances accuracy and computational complexity: computational complexity remains, by construction, independent of the number of switched environments.

4 Discussion

Surprise is a widely used concept describing a range of phenomena from unexpected events to behavioral responses. Existing approaches to quantifying surprise are either data-centered (30–32) or model-centered (29, 37) and may be objective (31, 32) or subjective (29, 30, 37) but are always linked to uncertainty. We emphasize that, in order for surprise to be behaviorally meaningful, it has to be defined for a *single* data sample such that an organism can respond to a single event. In contrast, information theoretic quantities, such as data entropy and mutual information, are usually defined as average quantities.

Based on our definition of surprise, we proposed a new framework for surprise-driven learning. There are two components to this framework: (i) a confidence-adjusted surprise measure to capture environmental statistics as well as subjective beliefs, (ii) the surprise-minimization learning rule, or SMiLe-rule, which dynamically adjusts the balance between new and old information without prior assumptions about the temporal statistics in the environment. Within this framework, the surprise is a single subject-specific variable that determines a subject’s propensity to modify existing beliefs. This algorithm is suitable for learning in complex environments that are either stable or undergo gradual or sudden changes. The latter are signaled by high surprise and result in placing more weight on new information. The significance of the proposed method is that it neither requires knowledge of the full Bayesian model of the environment nor any prior assumption about the temporal statistics in the environment. Moreover, it pro-

vides a simple framework that could potentially implemented in a neurally plausible way using probabilistic population codes (38, 39).

Relation to Bayesian surprise

One of the existing approaches for measuring surprise is *Bayesian surprise* (21, 29) which is generally defined as a distance or dissimilarity measure between prior and posterior beliefs. According to this measure, a data sample X is more surprising than a data sample X' if it causes a larger change in the subject's belief. One of the shortcomings of the Bayesian surprise is that it is computed only *after* learning (i.e., once we have changed our belief from prior to posterior). However, behavioral and neural responses indicate that surprise is concurrent with the unexpected event. Our working hypothesis is that the brain evaluates surprise even before recognition, inference or learning occurs. We thus need to evaluate surprise *before* we update our belief such that surprise may control learning rather than emerge from it. This property is fulfilled in the confidence-corrected surprise measure introduced in this paper.

Information content and Bayesian surprise are two distinct yet complementary approaches to measuring surprise. Information content is about *data* as it captures the inherent unexpectedness of a piece of data given a model. While its calculation is instantaneous and objective, it suffers from not knowing the true underlying parameter θ^* . Bayesian surprise is about a *model*. Since it measures the change in belief (i.e., in the model parameters), it is subjective and does not require knowing θ^* . However, it is computed only after learning, which is inconsistent with behavioral and neural data that suggest an instantaneous response to surprise. Our definition of raw surprise combines these two measures to use their complementary benefits and overcome their shortcomings (see Appendix **H**).

New versus old information

The proposed algorithm's performance is primarily driven by two features: (i) the algorithm adaptively increases the influence of new data on the belief update as a function of how surpris-

ing the data was; (ii) the algorithm increases model uncertainty in the face of surprising data thus increasing the influence of new data on current *and* future belief updates. The importance of the first point has been recognized and incorporated previously (2, 4). The second point is particularly worth noting: a surprising sample not only signals a potential change, it also signals that our current model may be wrong, so that we should be *less* certain about its accuracy. This increase in model uncertainty implies discounting the influence of past information in current and future belief updates.

Both humans and animals adaptively adjust the relative contribution of old and newly acquired data on learning (1–4) and rapidly adapt to changing environments (4–6). Standard Bayesian and reinforcement learning models in humans (40) or animals (41, 42) assume a stable environment and are slow to adapt to sudden changes in the environment. To quickly learn in dynamic environments, models need to include a way to detect and respond to sudden changes. A full (hierarchical) Bayesian approach works only if the subject is aware of the correct model of the task, (e.g., the time scale of change in the environment or the number of environments between which switches occur). Calculating the probability of a change point in a Gaussian estimation task (10), estimating the volatility of the environment in a reversal learning task (1), and dynamically forgetting the past information with a controlled time constant (43) are all examples of addressing learning in changing environments without explicit knowledge of the full Bayesian model.

In changing environments, hierarchical Bayesian models outperform the standard delta-rule with a fixed learning rate. However, hierarchical models either make assumptions about how fast the world is changing on average or about the underlying data generating process, in order to accurately detect a change in the environment. While our proposed surprise-based algorithm may not be theoretically optimal, it approximates the optimal (hierarchical) Bayesian solution without making any such assumption.

Model uncertainty

The ability of our proposed method to increase model uncertainty solves a common problem in standard Bayesian learning, namely, a model uncertainty or a learning rate approaching zero when the number of data samples increases. This is particularly prominent in Bayes' rule which is derived under the assumption of *stationarity* and which thus reduces posterior uncertainty in each step no matter how surprising a sample is. The SMiLe rule (7) guarantees that a small model uncertainty remains even after a long stationary period. This remaining uncertainty ensures that an organism can still detect a change even after having spent an extensive amount of time in a given environment (see Fig. 4C). One might argue, that reducing the learning rate to zero after extensive training is desirable under certain conditions as it corresponds to the well-documented phenomenon of overtraining whereby an organism no longer responds to changes in goal value. We would argue that this insensitivity is a consequence of behavioral control being handed over to the habitual system and thus to a different neural substrate (44–46).

Potential applications

Surprise minimization is a more general approach for learning than learning by reward prediction error. Recent approaches in reward learning suggest to use a scaled reward prediction error (8). A recurring problem in reward-based learning is the observation that subjects use different learning rates on a trial-by-trial basis even in stable environments. Researchers typically assume an average learning rate for fitting data. Note that in our approach, the learning rate varies naturally as a function of the last data point (as it should) while keeping the subject-specific parameter m constant.

Note that both confidence-corrected surprise and the SMiLe rule have wide-reaching implications outside the framework presented here. On the one hand, our surprise measure can not only *modulate* learning, but can be used as a *trigger* signal for an algorithm that needs to choose between several uncertain states or actions as is the case in change point detection (10, 43, 47),

memory and cluster formation (48), exploration/exploitation tradeoff (49, 50), novelty detection (51, 52), and network reset (53). On the other hand, the SMiLe-rule could add flexibility in learning and replace existing learning algorithms in scenarios where dynamically balancing old and new information is desired. This includes fitting γ to behavioral data without computing surprise or controlling γ by something other than surprise. Replacing the full Bayesian model of a learning task in changing environment with the SMiLe rule simplifies calculations, which makes the SMiLe-framework suitable to fit relevant parameters to behavioral data.

Experimental predictions.

There is ample evidence for a neural substrate of surprise. Existing measures of expectation violations such as absolute and variance-scaled reward prediction errors (54, 55), unexpected uncertainty (56) and risk prediction errors (9) have been linked to different neuromodulatory systems. Among those, the *noradrenergic system* has emerged as a prime candidate for signalling unexpected uncertainty and surprise: noradrenergic neurons respond to unexpected changes such as the presence of a novel stimulus, unexpected pairing of stimulus with a reinforcement during conditioning, and reversal of the contingencies (57–60). The P300 component of ERP (16, 17) which is associated with novelty (61) and surprise (18) is modulated by Noradrenaline (NE). It also modulates pupil size (62, 63) as a physiological response to surprise. The dynamics of noradrenergic system is fast enough to quickly respond to unexpected events (64–66), a functional requirement for surprise to control learning; see (53, 67, 68) for a review. We predict that, in experiments with changing environments, the activity of NE should exhibit a high correlation with the confidence-corrected surprise signal.

Note that Acetylcholine (ACh), on the other hand, is a candidate neuromodulator for encoding expected uncertainty (56) and thus is linked to the model uncertainty (although it might also be linked to other forms of uncertainty such as environmental stochasticity).

A variety of experimental findings are consistent with and can be explained by our definition

of confidence-corrected surprise and the SMiLe rule. It has been shown both theoretically (56) and empirically (69) that NE and ACh interact such that ACh sets a threshold for NE to indicate fundamental changes in the environment (56). This is consistent with our hypothesis that if an agent is uncertain about its current model of the world, unexpected events are perceived less surprising than when the agent is almost certain about its model (the idea behind the confidence-corrected surprise). The impairment of adaptation to contextual changes due to NE depletion (70) can be explained by incapability of subjects in responding to surprising events signaled by NE. The absence/suppression of ACh (low model uncertainty) implies little or no variability of the environment such that even small prediction error signals are perceived as surprising (71), consistent with the excessive activation of NE system in such situations.

Moreover, there is empirical evidence that NE and ACh both affect synaptic plasticity in the cortex and the hippocampus (69, 72), suppress cortical processing (73, 74) and facilitate information processing from thalamus to the cerebral cortex (75–77). This is consistent with our theory that surprise balances the influence of the newly acquired data (thalamocortical pathway) and old information (corticocortical pathway) during belief update.

In summary, we proposed a measure of surprise and a surprise-modulated belief update algorithm that can be used for modeling how humans and animals learn in changing environments. Our results suggest that the proposed method can approximate an optimal Bayesian learner, but with significantly reduced computational complexity. Our model provides a framework for future studies on learning with surprise. This include computational studies, such as how the proposed model can be neurally implemented, and neurobiological studies, such as unraveling the interaction between different neural circuits that are functionally involved in learning under surprise.

Acknowledgments

This project has been funded by the European Research Council (grant agreement no. 268 689, "MultiRules").

References and Notes

1. Timothy EJ Behrens, Mark W Woolrich, Mark E Walton, and Matthew FS Rushworth. Learning the value of information in an uncertain world. *Nature neuroscience*, 10(9):1214–1221, 2007.
2. Matthew R Nassar, Katherine M Rumsey, Robert C Wilson, Kinjan Parikh, Benjamin Heasly, and Joshua I Gold. Rational regulation of learning dynamics by pupil-linked arousal systems. *Nature neuroscience*, 15(7):1040–1046, 2012.
3. Lea K Krugel, Guido Biele, Peter NC Mohr, Shu-Chen Li, and Hauke R Heekeren. Genetic variation in dopaminergic neuromodulation influences the ability to rapidly and flexibly adapt decisions. *Proceedings of the National Academy of Sciences*, 106(42):17951–17956, 2009.
4. John M Pearce and Geoffrey Hall. A model for pavlovian learning: variations in the effectiveness of conditioned but not of unconditioned stimuli. *Psychological review*, 87(6):532, 1980.
5. Paul N Wilson, Patrick Boumphrey, and John M Pearce. Restoration of the orienting response to a light by a change in its predictive accuracy. *Quarterly Journal of Experimental Psychology: Section B*, 44(1):17–36, 1992.

6. Peter C Holland. Brain mechanisms for changes in processing of conditioned stimuli in pavlovian conditioning: Implications for behavior theory. *Animal Learning & Behavior*, 25(4):373–399, 1997.
7. Benjamin Y Hayden, Sarah R Heilbronner, John M Pearson, and Michael L Platt. Surprise signals in anterior cingulate cortex: neuronal encoding of unsigned reward prediction errors driving adjustment in behavior. *The Journal of Neuroscience*, 31(11):4178–4187, 2011.
8. Kerstin Preuschoff and Peter Bossaerts. Adding prediction risk to the theory of reward learning. *Annals of the New York Academy of Sciences*, 1104(1):135–146, 2007.
9. Kerstin Preuschoff, Steven R Quartz, and Peter Bossaerts. Human insula activation reflects risk prediction errors as well as risk. *The Journal of Neuroscience*, 28(11):2745–2752, 2008.
10. Matthew R Nassar, Robert C Wilson, Benjamin Heasly, and Joshua I Gold. An approximately bayesian delta-rule model explains the dynamics of belief updating in a changing environment. *The Journal of Neuroscience*, 30(37):12366–12378, 2010.
11. Elise Payzan-LeNestour and Peter Bossaerts. Risk, unexpected uncertainty, and estimation uncertainty: Bayesian learning in unstable settings. *PLoS computational biology*, 7(1):e1001048, 2011.
12. Ryan Prescott Adams and David JC MacKay. Bayesian online changepoint detection. *arXiv preprint arXiv:0710.3742*, 2007.
13. James Kalat. *Biological psychology*. Cengage Learning, 2012.
14. Eckhard H Hess and James M Polt. Pupil size as related to interest value of visual stimuli. *Science*, 132(3423):349–350, 1960.

15. Walter Bradford Cannon. The wisdom of the body. 1932.
16. JA Pineda, M Westerfield, BM Kronenberg, and J Kubrin. Human and monkey p3-like responses in a mixed modality paradigm: effects of context and context-dependent noradrenergic influences. *International Journal of Psychophysiology*, 27(3):223–240, 1997.
17. Pascal Missonnier, Richard Ragot, Christian Derouesné, David Guez, and Bernard Renault. Automatic attentional shifts induced by a noradrenergic drug in alzheimers disease: evidence from evoked potentials. *International journal of psychophysiology*, 33(3):243–251, 1999.
18. Piotr Jaskowski, Bernd Wauschkuhn, et al. Suspense and surprise: On the relationship between expectancies and p3. *Psychophysiology*, 31(4):359–369, 1994.
19. Antonio Kolossa, Bruno Kopp, and Tim Fingscheidt. A computational analysis of the neural bases of bayesian inference. *NeuroImage*, 106:222–237, 2015.
20. Adrienne L Fairhall, Geoffrey D Lewen, William Bialek, and Robert R de Ruyter van Steveninck. Efficiency and ambiguity in an adaptive neural code. *Nature*, 412(6849):787–792, 2001.
21. Laurent Itti and Pierre Baldi. Bayesian surprise attracts human attention. *Vision research*, 49(10):1295–1306, 2009.
22. Charan Ranganath and Gregor Rainer. Neural mechanisms for detecting and remembering novel events. *Nature Reviews Neuroscience*, 4(3):193–202, 2003.
23. Michael E Hasselmo. Neuromodulation: acetylcholine and memory consolidation. *Trends in cognitive sciences*, 3(9):351–359, 1999.

24. Gene V Wallenstein, Michael E Hasselmo, and Howard Eichenbaum. The hippocampus as an associator of discontiguous events. *Trends in neurosciences*, 21(8):317–323, 1998.
25. Yi Sun, Faustino Gomez, and Jürgen Schmidhuber. Planning to be surprised: Optimal bayesian exploration in dynamic environments. In *Artificial General Intelligence*, pages 41–51. Springer, 2011.
26. Daniel Y Little and Friedrich T Sommer. Learning in embodied action-perception loops through exploration. *arXiv preprint arXiv:1112.1125*, 2011.
27. Mikhail Frank, Jürgen Leitner, Marijn Stollenga, Alexander Förster, and Jürgen Schmidhuber. Curiosity driven reinforcement learning for motion planning on humanoids. *Frontiers in neurorobotics*, 7, 2013.
28. Karl Friston. The free-energy principle: a unified brain theory? *Nature Reviews Neuroscience*, 11(2):127–138, 2010.
29. Pierre Baldi and Laurent Itti. Of bits and wows: a bayesian theory of surprise with applications to attention. *Neural Networks*, 23(5):649–666, 2010.
30. Gunther Palm. *Novelty, information and surprise*. Springer, 2012.
31. Myron Tribus. Information theory as the basis for thermostatics and thermodynamics. *Journal of Applied Mechanics*, 28(1):1–8, 1961.
32. Claude Elwood Shannon. A mathematical theory of communication. *ACM SIGMOBILE Mobile Computing and Communications Review*, 5(1):3–55, 2001.
33. Richard Morris. Developments of a water-maze procedure for studying spatial learning in the rat. *Journal of neuroscience methods*, 11(1):47–60, 1984.

34. Sabine Gillner and Hanspeter A Mallot. Navigation and acquisition of spatial knowledge in a virtual maze. *Journal of Cognitive Neuroscience*, 10(4):445–463, 1998.
35. Andrew L Nelson, Edward Grant, John M Galeotti, and Stacey Rhody. Maze exploration behaviors using an integrated evolutionary robotics environment. *Robotics and Autonomous Systems*, 46(3):159–173, 2004.
36. Gianluigi Mongillo and Sophie Deneve. Online learning with hidden markov models. *Neural computation*, 20(7):1706–1716, 2008.
37. Laurent Itti and Pierre F Baldi. Bayesian surprise attracts human attention. In *Advances in neural information processing systems*, pages 547–554, 2005.
38. Wei Ji Ma, Jeffrey M Beck, Peter E Latham, and Alexandre Pouget. Bayesian inference with probabilistic population codes. *Nature neuroscience*, 9(11):1432–1438, 2006.
39. Jeffrey M Beck, Wei Ji Ma, Roozbeh Kiani, Tim Hanks, Anne K Churchland, Jamie Roitman, Michael N Shadlen, Peter E Latham, and Alexandre Pouget. Probabilistic population codes for bayesian decision making. *Neuron*, 60(6):1142–1152, 2008.
40. Joshua B Tenenbaum and Thomas L Griffiths. Structure learning in human causal induction. *Advances in neural information processing systems*, pages 59–65, 2001.
41. Peter Dayan, Sham Kakade, and P Read Montague. Learning and selective attention. *nature neuroscience*, 3:1218–1223, 2000.
42. Sham Kakade and Peter Dayan. Acquisition and extinction in autoshaping. *Psychological review*, 109(3):533, 2002.

43. Johannes Rüter, Nicolas Marcille, Henning Sprekeler, Wulfram Gerstner, and Michael H Herzog. Paradoxical evidence integration in rapid decision processes. *PLoS Comput Biol*, 8(2):e1002382, 2012.
44. Bernard W Balleine and John P O’Doherty. Human and rodent homologies in action control: corticostriatal determinants of goal-directed and habitual action. *Neuropsychopharmacology*, 35(1):48–69, 2010.
45. Bernard W Balleine and Anthony Dickinson. Goal-directed instrumental action: contingency and incentive learning and their cortical substrates. *Neuropharmacology*, 37(4):407–419, 1998.
46. Peter Redgrave, Manuel Rodriguez, Yoland Smith, Maria C Rodriguez-Oroz, Stephane Lehericy, Hagai Bergman, Yves Agid, Mahlon R DeLong, and Jose A Obeso. Goal-directed and habitual control in the basal ganglia: implications for parkinson’s disease. *Nature Reviews Neuroscience*, 11(11):760–772, 2010.
47. Robert C Wilson, Matthew R Nassar, and Joshua I Gold. A mixture of delta-rules approximation to bayesian inference in change-point problems. *PLoS computational biology*, 9(7):e1003150, 2013.
48. Samuel J Gershman and Yael Niv. Novelty and inductive generalization in human reinforcement learning. *Topics in cognitive science*, 7(3):391–415, 2015.
49. Jonathan D Cohen, Samuel M McClure, and J Yu Angela. Should i stay or should i go? how the human brain manages the trade-off between exploitation and exploration. *Philosophical Transactions of the Royal Society of London B: Biological Sciences*, 362(1481):933–942, 2007.

50. Marieke Jepma and Sander Nieuwenhuis. Pupil diameter predicts changes in the exploration–exploitation trade-off: evidence for the adaptive gain theory. *Journal of cognitive neuroscience*, 23(7):1587–1596, 2011.
51. Robert T Knight et al. Contribution of human hippocampal region to novelty detection. *Nature*, 383(6597):256–259, 1996.
52. Christopher M Bishop. Novelty detection and neural network validation. In *Vision, Image and Signal Processing, IEE Proceedings-*, volume 141, pages 217–222. IET, 1994.
53. Sebastien Bouret and Susan J Sara. Network reset: a simplified overarching theory of locus coeruleus noradrenaline function. *Trends in neurosciences*, 28(11):574–582, 2005.
54. Wolfram Schultz. Dopamine reward prediction-error signalling: a two-component response. *Nature Reviews Neuroscience*, 2016.
55. Wolfram Schultz. Neuronal reward and decision signals: from theories to data. *Physiological reviews*, 95(3):853–951, 2015.
56. Angela J Yu and Peter Dayan. Uncertainty, neuromodulation, and attention. *Neuron*, 46(4):681–692, 2005.
57. SJ Sara and M Segal. Plasticity of sensory responses of locus coeruleus neurons in the behaving rat: implications for cognition. *Progress in brain research*, 88:571–585, 1991.
58. Susan J Sara, Andrey Vankov, and Anne Hervé. Locus coeruleus-evoked responses in behaving rats: a clue to the role of noradrenaline in memory. *Brain research bulletin*, 35(5):457–465, 1994.

59. Andrey Vankov, Anne Hervé-Minvielle, and Susan J Sara. Response to novelty and its rapid habituation in locus coeruleus neurons of the freely exploring rat. *European Journal of Neuroscience*, 7(6):1180–1187, 1995.
60. G Aston-Jones, J Rajkowski, and P Kubiak. Conditioned responses of monkey locus coeruleus neurons anticipate acquisition of discriminative behavior in a vigilance task. *Neuroscience*, 80(3):697–715, 1997.
61. Emanuel Donchin, WALTER Ritter, W CHEYNE McCallum, et al. Cognitive psychophysiology: The endogenous components of the erp. *Event-related brain potentials in man*, pages 349–411, 1978.
62. Vincent D Costa and Peter H Rudebeck. More than meets the eye: the relationship between pupil size and locus coeruleus activity. *Neuron*, 89(1):8–10, 2016.
63. Kerstin Preuschoff, Bernard Marius t Hart, and Wolfgang Einhäuser. Pupil dilation signals surprise: evidence for noradrenalines role in decision making. *Front Neurosci*, 5:115, 2011.
64. J Rajkowski, P Kubiak, and G Aston-Jones. Locus coeruleus activity in monkey: phasic and tonic changes are associated with altered vigilance. *Brain research bulletin*, 35(5):607–616, 1994.
65. Edwin C Clayton, Janusz Rajkowski, Jonathan D Cohen, and Gary Aston-Jones. Phasic activation of monkey locus ceruleus neurons by simple decisions in a forced-choice task. *The Journal of neuroscience*, 24(44):9914–9920, 2004.
66. Sebastien Bouret and Susan J Sara. Reward expectation, orientation of attention and locus coeruleus-medial frontal cortex interplay during learning. *European Journal of Neuroscience*, 20(3):791–802, 2004.

67. Susan J Sara. The locus coeruleus and noradrenergic modulation of cognition. *Nature reviews neuroscience*, 10(3):211–223, 2009.
68. Gary Aston-Jones and Jonathan D Cohen. An integrative theory of locus coeruleus-norepinephrine function: adaptive gain and optimal performance. *Annu. Rev. Neurosci.*, 28:403–450, 2005.
69. Q Gu. Neuromodulatory transmitter systems in the cortex and their role in cortical plasticity. *Neuroscience*, 111(4):815–835, 2002.
70. Susan J Sara. Learning by neurones: role of attention, reinforcement and behaviour. *Comptes Rendus de l'Académie des Sciences-Series III-Sciences de la Vie*, 321(2):193–198, 1998.
71. DNC Jones and GA Higgins. Effect of scopolamine on visual attention in rats. *Psychopharmacology*, 120(2):142–149, 1995.
72. Mark F Bear and Wolf Singer. Modulation of visual cortical plasticity by acetylcholine and noradrenaline. 1986.
73. Fumitaka Kimura, Mitsuhiro Fukuda, and Tadaharu Tsumoto. Acetylcholine suppresses the spread of excitation in the visual cortex revealed by optical recording: possible differential effect depending on the source of input. *European Journal of Neuroscience*, 11(10):3597–3609, 1999.
74. Masayuki Kobayashi, Kazuyuki Imamura, Tokio Sugai, Norihiko Onoda, Masao Yamamoto, Shoji Komai, and Yasuyoshi Watanabe. Selective suppression of horizontal propagation in rat visual cortex by norepinephrine. *European Journal of Neuroscience*, 12(1):264–272, 2000.

75. Ziv Gil, Barry W Connors, and Yael Amitai. Differential regulation of neocortical synapses by neuromodulators and activity. *Neuron*, 19(3):679–686, 1997.
76. Michael E Hasselmo, Bradley P Wyble, and Gene V Wallenstein. Encoding and retrieval of episodic memories: role of cholinergic and gabaergic modulation in the hippocampus. *Hippocampus*, 6(6):693–708, 1996.
77. Candace Y Hsieh, Scott J Cruikshank, and Raju Metherate. Differential modulation of auditory thalamocortical and intracortical synaptic transmission by cholinergic agonist. *Brain research*, 880(1):51–64, 2000.
78. Bernhard Schölkopf and Alexander J Smola. *Learning with kernels: Support vector machines, regularization, optimization, and beyond*. MIT press, 2002.
79. David JC MacKay. *Information theory, inference and learning algorithms*. Cambridge university press, 2003.

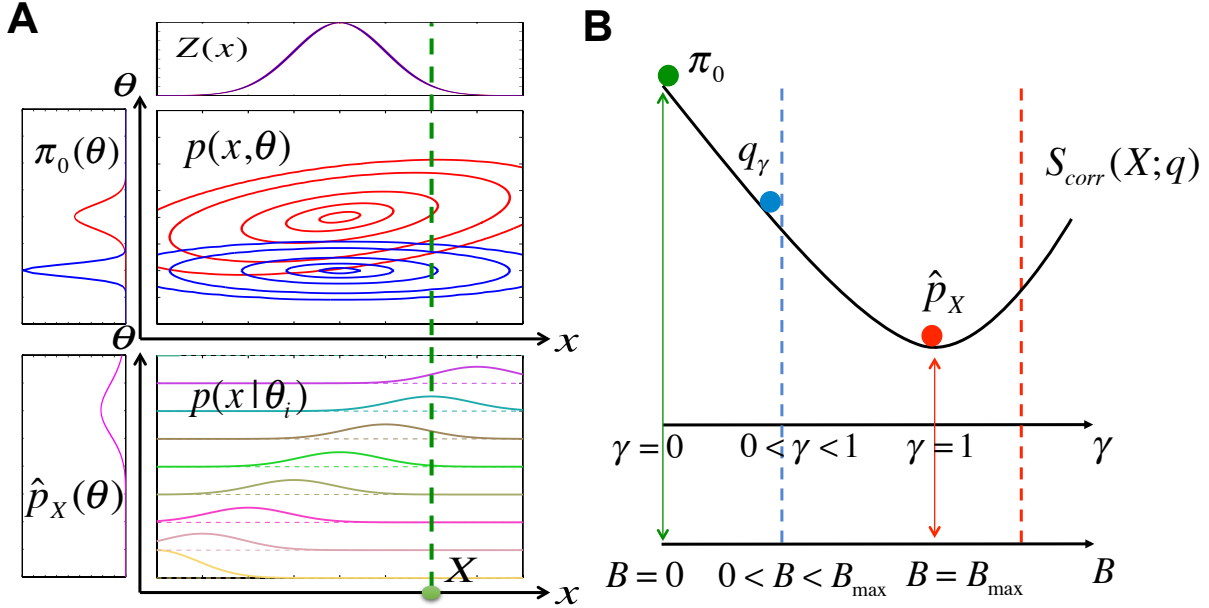


Figure 1: **A.** The impact of confidence on surprise. Top: Two distinct internal models (red and blue), described by joint distributions $p(x, \theta)$ (contour plots) over observable data x and model parameters θ , may have the same marginal distribution $Z(x) = \int_{\theta} p(x, \theta) d\theta$ (distributions along the x -axis coincide) but differ in the marginal distribution $\pi_0(\theta) = \int_x p(x, \theta) dx$ (distributions along the θ -axis). Surprise measures that are computed with respect to $Z(x)$ neglect the uncertainty as measured by the entropy $\mathcal{H}(\pi_0)$. Therefore, a given data sample X (green dot) may equally be surprising in terms of the raw surprise $S_{raw}(X)$ (1) but results in higher confidence-corrected surprise $S_{corr}(X)$ (3) for the blue as compared to the red model, because π_0 in the red model is wider (corresponding to a larger entropy) than in the blue model. Bottom: The scaled likelihood $\hat{p}_X(\theta)$ (magenta) for the "red" internal model is calculated by evaluating the conditional probability distribution functions $p(x|\theta_i)$ (specified by different color for each θ_i) at $x = X$ (intersection of dashed green line with colored curves). The confidence-corrected surprise $S_{corr}(X)$ is the KL divergence between $\hat{p}_X(\theta)$ (bottom, magenta) and $\pi_0(\theta)$ (top, red). **B.** Solutions to the (constraint) optimization problem (6). The objective function, i.e. the posterior surprise $S_{corr}(X; q)$ (black) for a given data sample X , is a parabolic landscape over γ where each γ corresponds to a unique posterior q_γ . Its global minimum is at $\gamma = 1$ (corresponding to $q_1 = \hat{p}_X$) which is equivalent to discarding all previously observed samples. The boundary B constrains the range of γ and thus the set of admissible posteriors. At $B = 0$ no change is allowed resulting in $\gamma = 0$ with a posterior equals to the prior π_0 (green). $B \geq B_{max} = D_{KL}[\hat{p}_X || \pi_0]$ (red dashed line) implies that we allow posteriors that are further away from the prior than the sample itself so the optimal solution is the scaled likelihood \hat{p}_X or $\gamma = 1$ as for the unconstrained problem. For $0 < B < B_{max}$ (blue dashed line) the objective function is minimized by q_γ (Eq. 7) that fulfills the constraint $D_{KL}[q_\gamma || \pi_0] = B$ with $0 < \gamma < 1$.

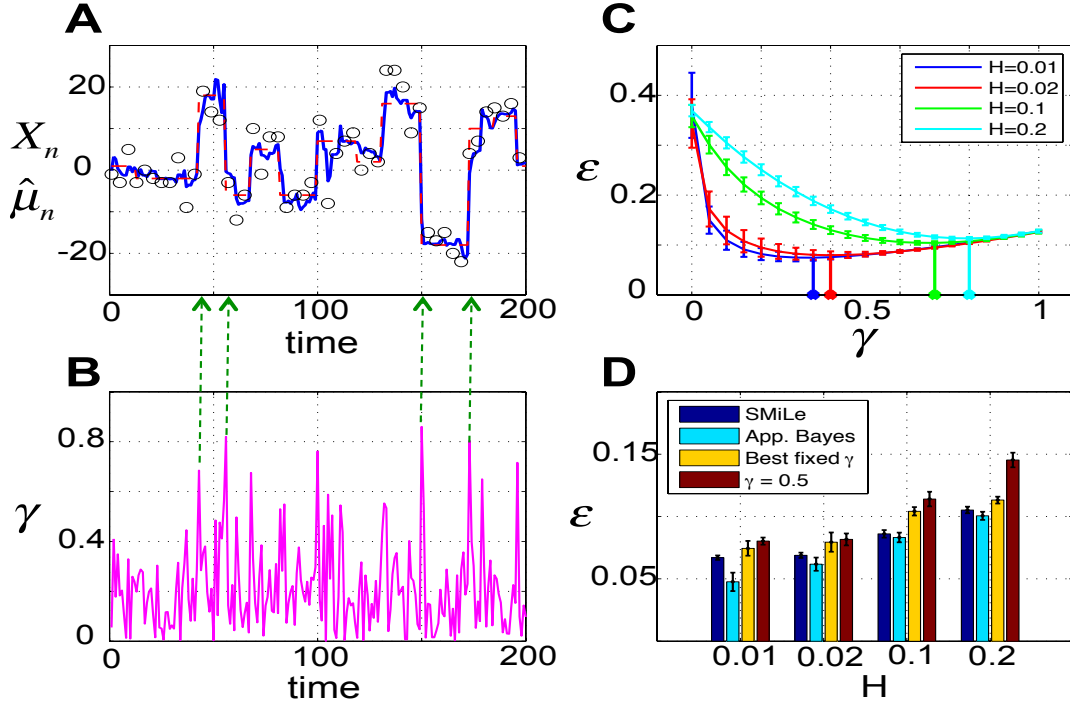


Figure 2: Gaussian mean estimation task. At each time step, a data sample X_n is independently drawn from a normal distribution whose underlying mean may change within the interval $[-20, 20]$ at unpredictable change points. On average, the underlying mean remains unchanged for 15 time steps corresponding to a hazard rate $H = 0.066$. The standard deviation of the distribution is fixed to 4 and is assumed to be known to the subject. **A.** Using a surprise-modulated belief update (algorithm 1), the estimated mean (blue) quickly approaches the true mean (dashed red) given observed samples (black circles). A few selected change points are indicated by green arrows. **B.** The weight factor γ (Eq. 11) (magenta) increases at the change points, resulting in higher influence of newly acquired data samples on the posterior mean. **C.** The estimation error ϵ per time step versus the weight factor $0 \leq \gamma \leq 1$ in the delta-rule method with constant γ for four different hazard rates. The minimum estimation error (for best fixed γ) is achieved by a γ (points on the horizontal axis) that decreases with the hazard rate, indicating that a bigger γ is preferred in volatile environments. Error bars indicate standard deviation over all trials and 50 episodes. **D.** For all models, the average estimation error ϵ increases with the hazard rate. Moreover, surprise-modulated belief update (SMiLe, dark blue) outperforms the delta-rule with the *best* fixed γ (Best fixed γ , yellow). The best fixed γ for each hazard rate corresponds to the learning rate that has minimal estimation error (indicated by points on the horizontal axis in sub-figure C). Although the surprise-modulated SMiLe rule performs worse than the approximate Bayesian delta-rule (10) (App. Bayes, light blue), the difference in the performance is not significant, except for the very small hazard rate of 0.01.

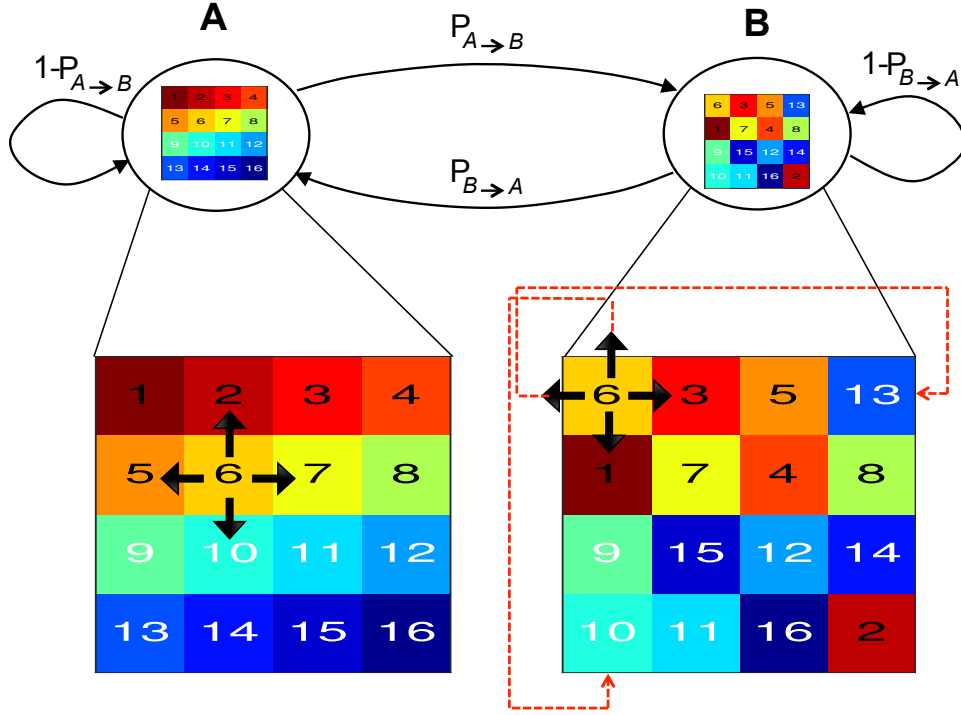


Figure 3: Maze exploration task. Environments \mathcal{A} (left) and \mathcal{B} (right) both consist of 16 rooms, but differ in topology. At each time step, one of the four available doors (up, down, right, left) in the current room (e.g. $s = 6$) is randomly opened (with probability 0.25). While the learning agent is in environment \mathcal{A} , the environment may change to \mathcal{B} with probability $P_{\mathcal{A} \rightarrow \mathcal{B}} \leq 0.1$ in the next time step of duration Δt . Similarly, $P_{\mathcal{B} \rightarrow \mathcal{A}}$ indicates the environment switches from \mathcal{B} to \mathcal{A} . Therefore, as the agent starts moving out of state $s = 6$, depending on the current environment and switch probabilities $P_{\mathcal{A} \rightarrow \mathcal{B}}$ and $P_{\mathcal{B} \rightarrow \mathcal{A}}$, it will end up in environment \mathcal{A} (i.e., $s' \in \{2, 10, 7, 5\}$) or \mathcal{B} (i.e., $s' \in \{10, 1, 3, 13\}$). The duration of a stay in environment \mathcal{A} is therefore exponentially distributed with mean $\tau_{\mathcal{A}} = \Delta t / P_{\mathcal{A} \rightarrow \mathcal{B}}$, where the parameter $\tau_{\mathcal{A}}$ determines the *time scale of stability* in environment \mathcal{A} , i.e., for larger $\tau_{\mathcal{A}}$ an agent has more time for adapting to \mathcal{A} after a change point. The *expected fraction of time spent in total* within environment \mathcal{A} is equal to $\psi_{\mathcal{A}} = P_{\mathcal{B} \rightarrow \mathcal{A}} / (P_{\mathcal{B} \rightarrow \mathcal{A}} + P_{\mathcal{A} \rightarrow \mathcal{B}})$. Note that $\tau_{\mathcal{A}}$ and $\psi_{\mathcal{A}}$ are two free parameters that we can change to study how the agent performs in different circumstances (e.g., see Fig. 7).

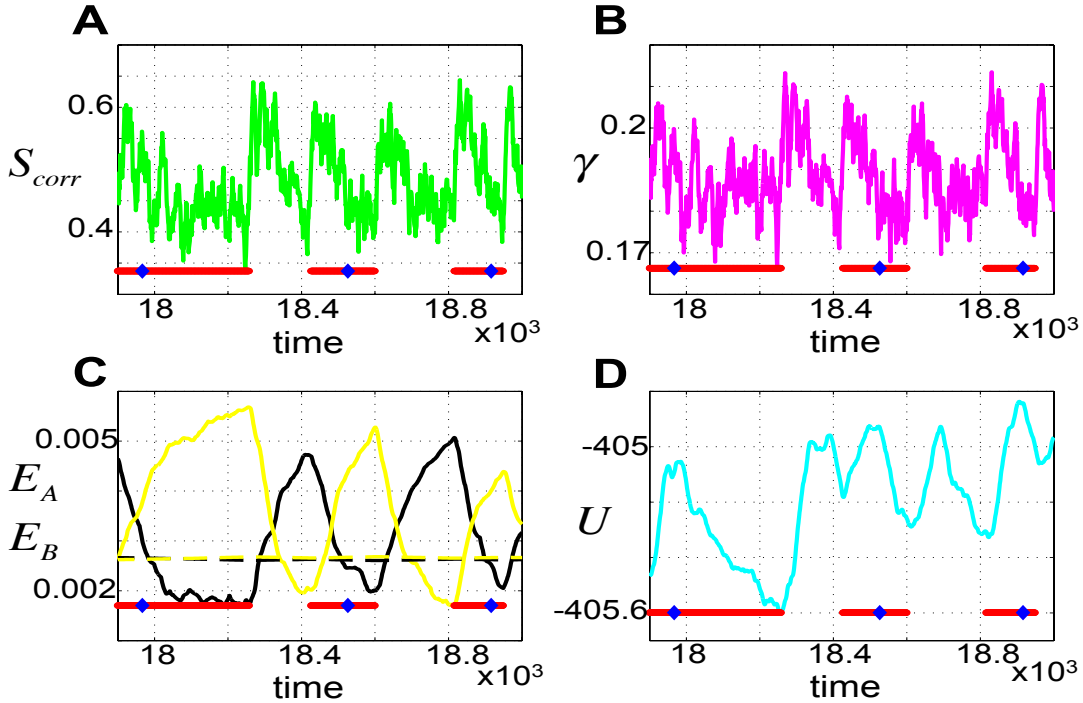


Figure 4: Time-series of relevant signals in the surprise-modulated belief update (algo 1 / algo 2) applied to the maze exploration task. All the curves have been smoothed with an exponential moving average (EMA) with a decay constant 0.1. The plots are shown for 1100 time steps (horizontal axis) toward the end of a simulation with 20000 time steps. The agent visits environments \mathcal{A} and \mathcal{B} *equally often* and spends *on average* 200 time steps in each environment before a switch occurs. Red bars indicate the time that the agent explores environment \mathcal{A} . Blue diamonds indicate 100 time steps after a change point from \mathcal{B} to \mathcal{A} . **A.** Confidence-corrected surprise S_{corr} (3) (green) increases at switch points and decreases (with fluctuations) till the next change point. **B.** The parameter γ (magenta) increases with the surprise at the change points and causes the next data samples to be more effective on belief update than the samples before the change point. **C.** The estimation errors for the transition matrix \hat{T} , $E_{\mathcal{A}}[t] = \|\hat{T}[t] - T_{\mathcal{A}}\|_2 = 256^{-1} \sum_{s,s'} [\hat{T}[t](s, s') - T_{\mathcal{A}}(s, s')]^2$ (solid black) and $E_{\mathcal{B}}[t] = \|\hat{T}[t] - T_{\mathcal{B}}\|_2$ (solid yellow) while in environment \mathcal{A} and \mathcal{B} , respectively, indicate a rapid adaptation to the new environment after the change points. The dashed black and yellow lines correspond to the estimation errors $E_{\mathcal{A}}$ and $E_{\mathcal{B}}$, respectively, when the naive Bayes rule (as a control experiment) is used for belief update. Naive Bayes rule converges to a stationary solution (no significant change in the estimation error after a switch of environment). **D.** The model uncertainty (light blue) increases for a few time steps following a change of the environment, an alert that the current model might be wrong. It then starts decreasing as the agent becomes more certain in the new environment.

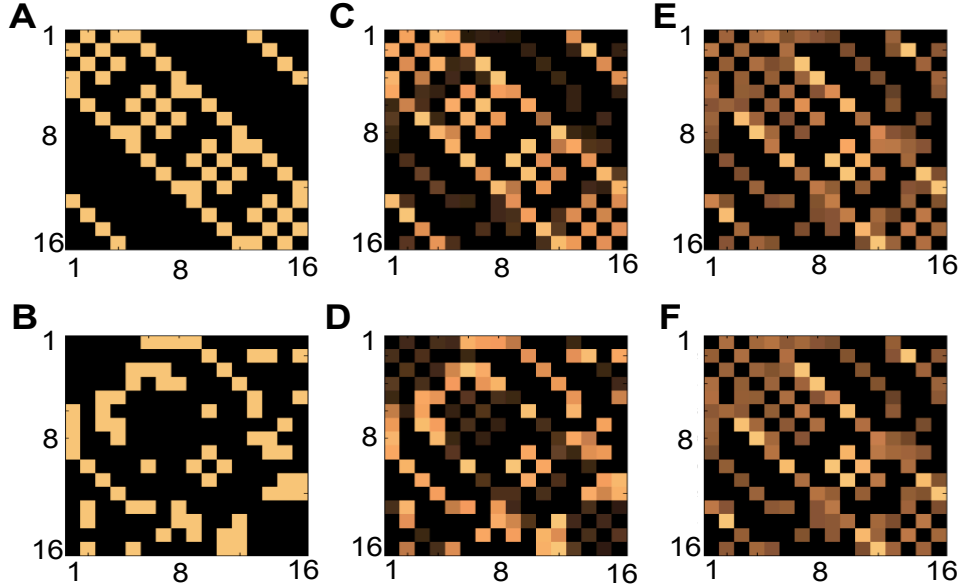


Figure 5: True and the estimated state transition probabilities in the maze exploration task. The color intensity for each entry (s, s') represents the probability of transition from a current state s (row) to a next state s' (column). **A.** The *true* state transition probability matrix $T_{\mathcal{A}}(s, s')$ in environment \mathcal{A} . Each row $T_{\mathcal{A}}(s, :)$ has only four non-zero entries (small squares with the light brown color) whose position indicate the neighboring rooms of state s in environment \mathcal{A} . Note that $\sum_{\tilde{s}} T_{\mathcal{A}}(s, \tilde{s}) = 1, \forall s$. **B.** The true state transition probability matrix $T_{\mathcal{B}}(s, s')$ for the environment \mathcal{B} which has a different topology compared to \mathcal{A} . **C.** The *estimated* state transition probability matrix $\hat{T}_{\mathcal{A}}$ when the surprise-modulated algorithm 2 is used for belief update. $\hat{T}_{\mathcal{A}} = K^{-1} \sum_{k=1}^K \hat{T}[t_{\mathcal{B} \rightarrow \mathcal{A}}^k + 100]$ is calculated by averaging the estimated transition matrix $\hat{T}[t]$ at 100 time steps after each of K change points $t_{\mathcal{B} \rightarrow \mathcal{A}}^k$. Here, $t_{\mathcal{B} \rightarrow \mathcal{A}}^k$ denotes the k -th time that the environment is changed from \mathcal{B} to \mathcal{A} and *has remained unchanged* for at least the next 100 time steps (relevant time points are indicated by blue diamonds in Fig. 4). The similarity between $\hat{T}_{\mathcal{A}}$ and $T_{\mathcal{A}}$ indicates that algorithm 2 enables the agent to quickly adapt to environment \mathcal{A} once a switch from \mathcal{B} to \mathcal{A} occurs. **D.** The estimated transition matrix $\hat{T}_{\mathcal{B}}$ (similarly defined as $\hat{T}_{\mathcal{A}}$ but for environment \mathcal{B}) when algorithm 2 is used for belief update. Note its similarity to the true matrix $T_{\mathcal{B}}$. **E-F.** The estimated state transition probability matrices $\tilde{T}_{\mathcal{A}}$ (up) and $\tilde{T}_{\mathcal{B}}$ (down) when the naive Bayesian method (as a control experiment) is used for belief update. A Bayesian agent does not adapt well to the new environment after a switch occurs, because it learns a weighted average of true transition matrices $T_{\mathcal{A}}$ and $T_{\mathcal{B}}$, where the weight is proportional to the fraction of time spent in each environment. Since both environments are visited equally in this experiment, the estimated quantities approach $(T_{\mathcal{A}} + T_{\mathcal{B}})/2$.

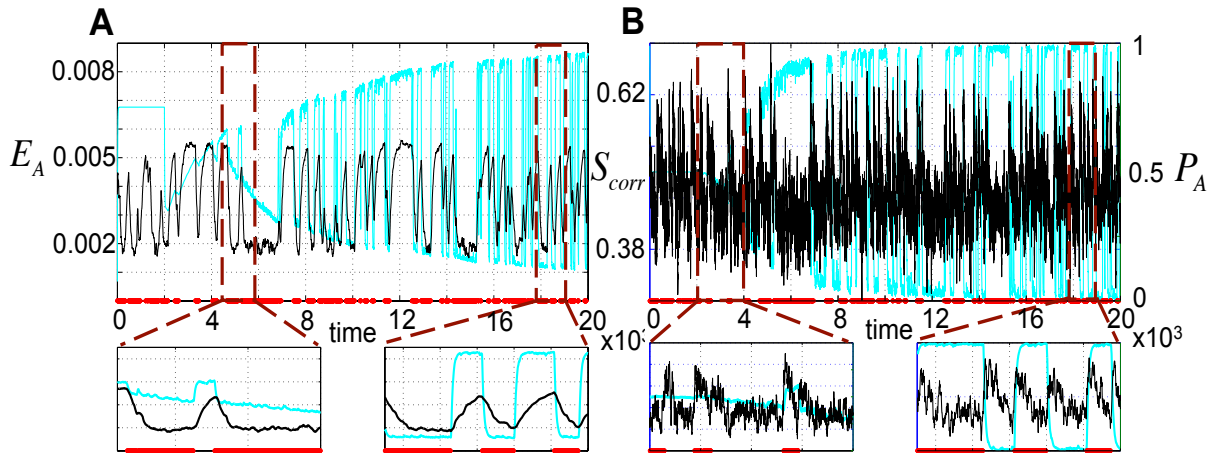


Figure 6: Comparison of surprise-modulated belief update with an online EM algorithm for the hierarchical Bayesian model. **A.** The estimation error E_A (vertical axis) of state transition probabilities within environment \mathcal{A} versus time (horizontal axis), for surprise-modulated belief update (black) and online EM learner (blue). Bottom plots depict zooms during the early (left) and late (right) phases of a simulation of 20000 time steps. In the early phase of learning (bottom left), the surprise-modulated belief update enables the agent to quickly learn model parameters after a switch to environment \mathcal{A} (indicated by red bars). In the late phase of learning (right), however, the online EM algorithm adapts to the new environment faster and more accurately than the surprise-modulated belief update. **B.** The inferred probability P_A of being in environment \mathcal{A} (blue, right vertical axis) used in the online EM algorithm, and the confidence-corrected surprise S_{corr} (black, left vertical axis) used in the surprise-modulated belief update.

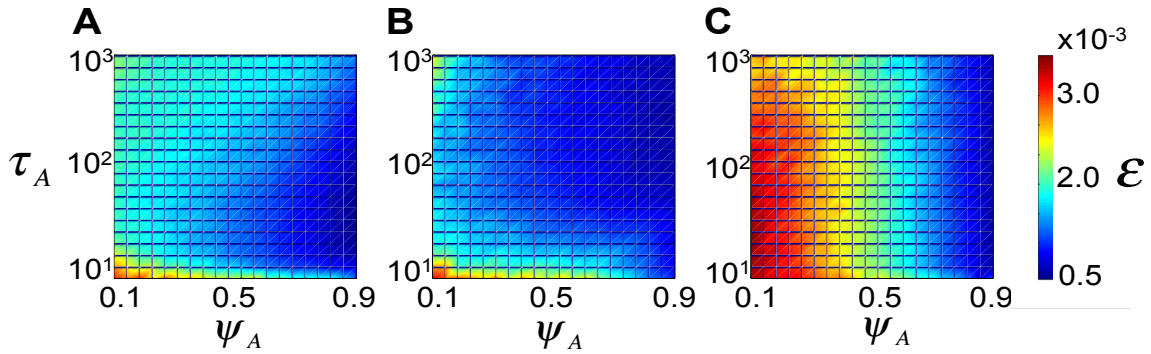


Figure 7: The estimation error ϵ in the maze exploration task, as a function of (1) the average time spent in environment \mathcal{A} before a switch to environment \mathcal{B} ($\tau_{\mathcal{A}} = \Delta t/p_{\mathcal{A} \rightarrow \mathcal{B}}$, vertical axis) and (2) the fraction of time spent in environment \mathcal{A} ($\psi_{\mathcal{A}} = P_{\mathcal{B} \rightarrow \mathcal{A}}/(P_{\mathcal{B} \rightarrow \mathcal{A}} + P_{\mathcal{A} \rightarrow \mathcal{B}})$, horizontal axis). **A.** The average estimation error (of state transition probabilities), 64 time steps after a switch from \mathcal{B} to \mathcal{A} , when surprise-modulated belief update (algorithm 2) is used for learning. The spread of blue color (lower estimation error) illustrates that surprise-modulated belief update enables an agent to quickly adapt to the environment visited after a switch. For each pair $(\tau_{\mathcal{A}}, \psi_{\mathcal{A}})$, the simulation is repeated for 20 episodes, each consisting of 20000 time steps. In each episode a different rearrangement of rooms for building environment \mathcal{B} is used to make sure that the result is not biased by a specific choice of this environment. **B.** The average estimation error when the online EM algorithm is used for learning the hierarchical statistical model. **C.** The average estimation error when naive Bayesian learner is used for belief update. The estimation error for this model is mainly determined by the fraction of time spent in environment \mathcal{A} (i.e., $\psi_{\mathcal{A}}$). The estimation error decreases with the time spent in environment \mathcal{A} , regardless of the time scale of stability determined by $\tau_{\mathcal{A}}$.

Appendix A: The scaled likelihood is the posterior belief under a flat prior.

Assume that all model parameters θ must stay in some bounded convex interval of surface A . Given a data sample X , the posterior belief $p^{flat}(\theta|X)$ about the model parameters θ (derived by the Bayes rule) under the assumption of a flat prior $\hat{\pi}_0(\theta) = 1/A$ is:

$$p^{flat}(\theta|X) = \frac{p(X|\theta)\hat{\pi}_0(\theta)}{\int_{\Theta} p(X|\theta)\hat{\pi}_0(\theta) d\theta} = \frac{p(X|\theta)}{\int_{\Theta} p(X|\theta) d\theta} = \frac{p(X|\theta)}{\|p_X\|} = \hat{p}_X(\theta). \quad (12)$$

Therefore, the scaled likelihood $\hat{p}_X(\theta)$ and the prior belief $\pi_0(\theta)$ both belong to the space of well-defined probability density functions for the model parameters θ . The KL divergence between the two distributions is the confidence-corrected surprise.

Appendix B: Derivation of the SMiLe rule

We note that the KL divergence $D_{KL}[a||b]$ is convex with respect to the first argument, i.e., a . Therefore, both the objective function $S_{corr}(X; q)$ (3) and the constraint $D_{KL}[q||\pi_0] \leq B$ in the optimization problem (6) are convex with respect to q which ensures the existence of the optimal solution.

In all appendices, small numbers above an equality sign refers to equations in the main text or other appendices.

We solve the constraint optimization by introducing a non-negative Lagrange multiplier $\lambda^{-1} \geq 0$ and a Lagrangian

$$\begin{aligned} \mathbb{L}(q, \lambda) &= S_{corr}(X; q) - \frac{1}{\lambda}(B - D_{KL}[q||\pi_0]) \\ &\stackrel{(2)}{=} \left\langle -\ln p(X|\theta) + \ln q(\theta) + \frac{1}{\lambda} \ln \frac{q(\theta)}{\pi_0(\theta)} \right\rangle_q - \frac{B}{\lambda} + \ln \|p\|, \end{aligned} \quad (13)$$

where $\langle \cdot \rangle_q$ denotes the average with respect to q . Similar to the standard approach that is used in support vector machines (78), the Lagrangian \mathbb{L} defined in (13) must be minimized with respect

to the primal variable q and maximized with respect to the dual variable λ (i.e., a saddle point must be found). Therefore the constraint problem (6) can be expressed as

$$\arg \min_q \max_{\lambda \geq 0} \mathbb{L}(q, \lambda). \quad (14)$$

By taking the derivative of \mathbb{L} with respect to q and setting it equal to zero,

$$\frac{\partial \mathbb{L}}{\partial q} = -\ln p(X|\theta) + [1 + \ln q(\theta)] + \frac{1}{\lambda} [1 + \ln \frac{q(\theta)}{\pi_0(\theta)}] = 0, \quad (15)$$

we find that the Lagrangian (13) is minimized by (7), i.e., $q(\theta) \propto p(X|\theta)^\gamma \pi_0(\theta)^{1-\gamma}$, where

$$0 \leq \gamma = \frac{\lambda}{\lambda + 1} \leq 1, \quad (16)$$

is determined by Lagrange multiplier λ . Note that the constant $Z(X; \gamma)$ in (7) follows from straight normalization of $q(\theta)$ to integral one.

Appendix C: The impact of a data sample X on belief update increases with γ in the SMiLe rule.

To prove the statement above we need to show that the impact function $\Delta S_{corr}(X; L)$ (5), where L is replaced by the SMiLe rule (7), increases with the parameter γ . In the following we show that the first derivative of the impact function with respect to γ is always non-negative.

But first we need to evaluate the derivative of $q_\gamma(\theta)$, Eq. (7), with respect to γ :

$$\begin{aligned} \frac{\partial}{\partial \gamma} q_\gamma(\theta) &= \frac{1}{Z(X; \gamma)} \frac{\partial}{\partial \gamma} [p(X|\theta)^\gamma \pi_0(\theta)^{1-\gamma}] + p(X|\theta)^\gamma \pi_0(\theta)^{1-\gamma} \frac{\partial}{\partial \gamma} \left[\frac{1}{Z(X; \gamma)} \right] \\ &= \frac{1}{Z(X; \gamma)} [p(X|\theta)^\gamma \pi_0(\theta)^{1-\gamma} \ln \frac{p(X|\theta)}{\pi_0(\theta)}] - \frac{p(X|\theta)^\gamma \pi_0(\theta)^{1-\gamma}}{Z(X; \gamma)^2} \frac{\partial}{\partial \gamma} [Z(X; \gamma)] \\ &= q_\gamma(\theta) \ln \frac{p(X|\theta)}{\pi_0(\theta)} - q_\gamma(\theta) \frac{1}{Z(X; \gamma)} \left[\int_{\Theta} \ln \frac{p(X|\theta)}{\pi_0(\theta)} p(X|\theta)^\gamma \pi_0(\theta)^{1-\gamma} d\theta \right] \\ &= q_\gamma(\theta) \left(\ln \frac{p(X|\theta)}{\pi_0(\theta)} - \left\langle \ln \frac{p(X|\theta)}{\pi_0(\theta)} \right\rangle_{q_\gamma} \right). \end{aligned} \quad (17)$$

Note also that

$$\int_{\Theta} \frac{\partial}{\partial \gamma} q_{\gamma}(\theta) d\theta \stackrel{(17)}{=} \int_{\Theta} q_{\gamma}(\theta) \left(\ln \frac{p(X|\theta)}{\pi_0(\theta)} - \left\langle \ln \frac{p(X|\theta)}{\pi_0(\theta)} \right\rangle_{q_{\gamma}} \right) d\theta = 0. \quad (18)$$

The derivative of $\Delta S_{corr}(X, \gamma)$ with respect to γ then becomes

$$\begin{aligned} \frac{\partial}{\partial \gamma} \Delta S_{corr}(X, L(\gamma)) &= -\frac{\partial}{\partial \gamma} S_{corr}(X, q_{\gamma}) \stackrel{(3)}{=} \int_{\Theta} \frac{\partial}{\partial \gamma} \left[q_{\gamma} \ln \frac{p(X|\theta)}{q_{\gamma}(\theta)} \right] d\theta \\ &= \int_{\Theta} \left(\ln \frac{p(X|\theta)}{q_{\gamma}(\theta)} \frac{\partial}{\partial \gamma} [q_{\gamma}(\theta)] + q_{\gamma}(\theta) \frac{\partial}{\partial \gamma} \left[\ln \frac{p(X|\theta)}{q_{\gamma}(\theta)} \right] \right) d\theta \\ &= \int_{\Theta} \left(\ln \frac{p(X|\theta)}{q_{\gamma}(\theta)} - 1 \right) \frac{\partial}{\partial \gamma} [q_{\gamma}(\theta)] d\theta \\ &\stackrel{(7)}{=} \int_{\Theta} \left((1 - \gamma) \ln \frac{p(X|\theta)}{\pi_0(\theta)} + \ln Z(X; \gamma) - 1 \right) \frac{\partial}{\partial \gamma} [q_{\gamma}(\theta)] d\theta \\ &\stackrel{(18)}{=} (1 - \gamma) \int_{\Theta} \left(\ln \frac{p(X|\theta)}{\pi_0(\theta)} \right) \frac{\partial}{\partial \gamma} [q_{\gamma}(\theta)] d\theta \\ &\stackrel{(17)}{=} (1 - \gamma) \int_{\Theta} \left(\ln \frac{p(X|\theta)}{\pi_0(\theta)} \right) \left(\ln \frac{p(X|\theta)}{\pi_0(\theta)} - \left\langle \ln \frac{p(X|\theta)}{\pi_0(\theta)} \right\rangle_{q_{\gamma}} \right) q_{\gamma}(\theta) d\theta \\ &= (1 - \gamma) \left(\int_{\Theta} \left(\ln \frac{p(X|\theta)}{\pi_0(\theta)} \right)^2 q_{\gamma}(\theta) d\theta - \left\langle \ln \frac{p(X|\theta)}{\pi_0(\theta)} \right\rangle_{q_{\gamma}} \int_{\Theta} \ln \frac{p(X|\theta)}{\pi_0(\theta)} q_{\gamma}(\theta) d\theta \right) \\ &= (1 - \gamma) \left(\left\langle \left(\ln \frac{p(X|\theta)}{q_{\gamma}(\theta)} \right)^2 \right\rangle_{q_{\gamma}} - \left(\left\langle \ln \frac{p(X|\theta)}{\pi_0(\theta)} \right\rangle_{q_{\gamma}} \right)^2 \right) \\ &= (1 - \gamma) \text{var} \left[\ln \frac{p(X|\theta)}{\pi_0(\theta)} \right] \geq 0. \end{aligned} \quad (19)$$

Appendix D: A larger reduction in the surprise implies a bigger change in belief.

The minimal value of the Lagrangian $\mathbb{L}(q, \lambda)$ (13) that is achieved by the posterior q_γ (7), obtained by the SMiLe rule, is equal to

$$\begin{aligned}
\mathbb{L}(q_\gamma, \lambda) &\stackrel{(13)}{=} \left\langle -\ln p(X|\theta) + \ln q_\gamma(\theta) + \frac{1}{\lambda} \ln \frac{q_\gamma(\theta)}{\pi_0(\theta)} \right\rangle_{q_\gamma} \overbrace{-\frac{B}{\lambda} + \ln \|p\|}^{=C} \\
&= \left\langle -\ln p(X|\theta) + \ln \frac{p(X|\theta)^\gamma \pi_0(\theta)^{1-\gamma}}{Z(X; \gamma)} + \frac{1}{\lambda} \ln \frac{p(X|\theta)^\gamma \pi_0(\theta)^{1-\gamma}}{Z(X; \gamma) \pi_0(\theta)} \right\rangle_{q_\gamma} + C \\
&= \left\langle \left(-1 + \gamma + \frac{\gamma}{\lambda}\right) \ln p(X|\theta) + \left(1 - \gamma - \frac{\gamma}{\lambda}\right) \ln \pi_0 - \left(1 + \frac{1}{\lambda}\right) \ln Z(X; \gamma) \right\rangle_{q_\gamma} + C \\
&= \left\langle \left(-1 + \gamma \left(1 + \frac{1}{\lambda}\right)\right) \ln \frac{p(X|\theta)}{\pi_0(\theta)} - \left(1 + \frac{1}{\lambda}\right) \ln Z(X; \gamma) \right\rangle_{q_\gamma} + C \\
&= -\frac{1}{\gamma} \ln Z(X; \gamma) + C. \tag{20}
\end{aligned}$$

Note that we used the equality $\frac{1}{\gamma} = 1 + \frac{1}{\lambda}$ (Eq. 16) in the last line of Eq. (20). If the minimizer q_γ is approximated by any other distribution function q , then its corresponding functional value $\mathbb{L}(q, \lambda)$ differs from its minimal value $\mathbb{L}(q_\gamma, \lambda)$ (20) in proportion to the KL divergence $D_{KL}[q||q_\gamma]$. This is because,

$$\begin{aligned}
\mathbb{L}(q, \lambda) - \mathbb{L}(q_\gamma, \lambda) &\stackrel{(13),(20)}{=} \left\langle -\ln p(X|\theta) + \ln q(\theta) + \frac{1}{\lambda} \ln \frac{q(\theta)}{\pi_0(\theta)} \right\rangle_q + \frac{1}{\gamma} \ln Z(X; \gamma) \\
&= \frac{1}{\gamma} \left\langle -\ln p(X|\theta)^\gamma + \ln q(\theta)^\gamma + \ln \left(\frac{q(\theta)}{\pi_0(\theta)}\right)^{\frac{\gamma}{\lambda}} + \ln Z(X; \gamma) \right\rangle_q \\
&= \frac{1}{\gamma} \left\langle \ln \frac{q(\theta)^{\gamma(1+\frac{1}{\lambda})} Z(X; \gamma)}{p(X|\theta)^\gamma \pi_0(\theta)^{\frac{\gamma}{\lambda}}} \right\rangle_q = \frac{1}{\gamma} \left\langle \ln \frac{q(\theta) Z(X; \gamma)}{p(X|\theta)^\gamma \pi_0(\theta)^{1-\gamma}} \right\rangle_q \\
&= \frac{1}{\gamma} D_{KL}[q||q_\gamma]. \tag{21}
\end{aligned}$$

Replacing q with π_0 in (21) follows the impact function $\Delta S_{corr}(X, L)$ (5) to be,

$$\begin{aligned}
\Delta S_{corr}(X, L(\gamma)) &= S_{corr}(X; \pi_0) - S_{corr}(X; q_\gamma) \\
&\stackrel{(13)}{=} \mathbb{L}(\pi_0, \lambda) + \frac{1}{\lambda}B - \mathbb{L}(q_\gamma, \lambda) - \frac{1}{\lambda}(B - D_{KL}[q_\gamma||\pi_0]) \\
&= \mathbb{L}(\pi_0, \lambda) - \mathbb{L}(q_\gamma, \lambda) + \frac{1}{\lambda}D_{KL}[q_\gamma||\pi_0] \\
&\stackrel{(21)}{=} \frac{1}{\gamma}D_{KL}[\pi_0||q_\gamma] + \frac{1}{\lambda}D_{KL}[q_\gamma||\pi_0] \\
&\stackrel{(16)}{=} \frac{1}{\gamma}D_{KL}[\pi_0||q_\gamma] + \left(\frac{1}{\gamma} - 1\right)D_{KL}[q_\gamma||\pi_0] \geq 0. \tag{22}
\end{aligned}$$

Therefore, the reduction in the posterior surprise is related to the belief changes $D_{KL}[\pi_0||q_\gamma]$ and $D_{KL}[q_\gamma||\pi_0]$ via Eq. (22). Note that the equality in (22) holds if and only if there is no change in the prior belief, i.e., if $q_\gamma = \pi_0$. This happens only if $\gamma = 0$ which is equivalent to the full neglect of the new data point in deriving the posterior belief.

Appendix E: The SMiLe rule for beliefs described by Gaussian distribution

Suppose we have drawn $n - 1$ samples X_1, \dots, X_{n-1} from a Gaussian distribution of known variance σ_x^2 , but unknown mean. The empirical mean after $n - 1$ samples is $\hat{\mu}_{n-1}$.

Assume that the current belief about the mean μ is a normal distribution, i.e., $\pi_0(\mu) \sim \mathcal{N}(\hat{\mu}_{n-1}, \sigma_{n-1}^2)$. Since the likelihood of receiving a new sample X_n is also normal, i.e., $p(X_n|\mu) \sim \mathcal{N}(\mu, \sigma_x^2)$, the posterior belief obtained by the SMiLe rule (7) is

$$\begin{aligned}
q_\gamma(\mu) &\propto \left(\exp\left(-\frac{(X_n - \mu)^2}{2\sigma_x^2}\right) \right)^\gamma \left(\exp\left(-\frac{(\mu - \hat{\mu}_{n-1})^2}{2\sigma_{n-1}^2}\right) \right)^{1-\gamma} \\
&\propto \exp\left(-\frac{(X_n - \mu)^2}{2(\sigma'_x)^2}\right) \exp\left(-\frac{(\mu - \hat{\mu}_{n-1})^2}{2(\sigma'_{n-1})^2}\right), \tag{23}
\end{aligned}$$

where $(\sigma'_x)^2 = \sigma_x^2/\gamma$ and $(\sigma'_{n-1})^2 = \sigma_{n-1}^2/(1 - \gamma)$. Because the product of two Gaussians is a Gaussian, we arrive at a posterior distribution $q_\gamma \sim \mathcal{N}(\hat{\mu}_n, \sigma_n^2)$ with the mean $\hat{\mu}_n = w_n X_n + (1 - w_n)\hat{\mu}_{n-1}$ (with $w_n = \frac{(\sigma'_{n-1})^2}{(\sigma'_x)^2 + (\sigma'_{n-1})^2}$), and the variance $\sigma_n^2 = \left(\frac{1}{(\sigma'_x)^2} + \frac{1}{(\sigma'_{n-1})^2}\right)^{-1}$; see (79) for the exact derivation. Assuming $\sigma_{n-1}^2 = \sigma_x^2$, then $w_n = \gamma$.

Moreover, we can evaluate the confidence-corrected surprise to be

$$S_{corr}(X_n; \pi_0) = D_{KL}[\mathcal{N}(\hat{\mu}_{n-1}, \sigma_{n-1}^2) || \mathcal{N}(X_n, \sigma_x^2)] = \frac{(X_n - \hat{\mu}_{n-1})^2}{2\sigma_x^2}. \quad (24)$$

Note that in Eq. (24), we used the following formula (with an assumption $\sigma_x^2 = \sigma_{n-1}^2$),

$$D_{KL}[\mathcal{N}(a_1, b_1^2) || \mathcal{N}(a_2, b_2^2)] = \frac{(a_1 - a_2)^2}{2b_2^2} + \frac{1}{2} \left(\frac{b_1^2}{b_2^2} - 1 - \ln \frac{b_1^2}{b_2^2} \right). \quad (25)$$

Appendix F: The SMiLe rule for beliefs described by Dirichlet distribution

Assume that the current belief about the probability of transition from state $s \in \{1, 2, \dots, D\}$ to all $D - 1$ possible next states $\check{s} \in \{1, 2, \dots, D\} \setminus s$ is described by a Dirichlet distribution $\pi_0(\boldsymbol{\theta}_s) \propto \prod_{\check{s}} \theta(s, \check{s})^{\alpha(s, \check{s})-1}$ parametrized by $\boldsymbol{\alpha}_s = \alpha(s, :)$. Here, $\boldsymbol{\theta}_s = \theta(s, :)$ denotes a *vector* of random variable $\theta(s, \check{s})$ that determines the probability of transition from s to \check{s} , i.e., $0 \leq \theta(s, \check{s}) \leq 1$ and $\sum_{\check{s}} \theta(s, \check{s}) = 1$. The likelihood function for an occurred transition $X : s \rightarrow s'$ is $p(X | \boldsymbol{\theta}_s) = \theta(s, s') = \prod_{\check{s}} \theta(s, \check{s})^{[\check{s}=s']}$, where $[\cdot]$ denotes the Iverson bracket. Therefore, the posterior belief $q_\gamma(\boldsymbol{\theta}_s)$ obtained by the SMiLe rule (7),

$$q_\gamma(\boldsymbol{\theta}_s) \propto \left(\prod_{\check{s}} \theta(s, \check{s})^{[\check{s}=s']} \right)^\gamma \cdot \left(\prod_{\check{s}} \theta(s, \check{s})^{\alpha(s, \check{s})-1} \right)^{1-\gamma} \propto \prod_{\check{s}} \theta(s, \check{s})^{\beta(s, \check{s})-1}, \quad (26)$$

is again a Dirichlet distribution parametrized by $\beta(s, \check{s}) = (1 - \gamma)\alpha(s, \check{s}) + \gamma(1 + [\check{s} = s'])$.

The probability $\hat{T}[t](s, s')$ of transition from s to s' at time step t is estimated by $\hat{T}[t](s, s') = \frac{\alpha[t](s, s') - 1 + \epsilon}{\sum_{\check{s}} (\alpha[t](s, \check{s}) - 1 + \epsilon)}$, where $\alpha[t](s, \check{s})$ denotes the updated model parameter at time step t . Here, $\epsilon > 0$ is a very small number which prevents the denominator to be zero.

Appendix G: The online EM algorithm for the maze-exploration task

The online EM algorithm, presented in (36), is an estimation algorithm for unknown parameters of a hidden Markov model (HMM). For the maze-exploration task we adapted the method presented in (36) such that the transition probability to a new room also depends on the previously visited room (and not just the current environment). The HMM of the maze-exploration

task consists of two sets of unknown parameters: (i) a set $\mathbf{P} = [P_{ij}]_{2 \times 2}$ of (unknown) switch probabilities from environment i to j (where we use 1 for environment \mathcal{A} and 2 for environment \mathcal{B}), and (ii) a set $\mathbf{T} = [T_{jss'}]_{2 \times 16 \times 16}$ of state transition probabilities, where $T_{jss'}$ denotes the probability of transition from state s to state s' within environment j . The set of all unknown parameters is denoted by $\Theta \equiv (\mathbf{P}, \mathbf{T})$.

At each time step t , we estimate the probability $q_l^t = P(E_t = l | s_{0 \rightarrow t})$ of being in environment $E_t = l \in \{1, 2\}$, given all previous state transitions $s_{0 \rightarrow t} = \{s_0, s_1, \dots, s_t\}$. The probability q_l^t can be recursively calculated by

$$\hat{q}_l^t = \sum_m \hat{q}_m^{t-1} \gamma_{ml}^t, \quad (27)$$

where $\gamma_{ml}^t = \frac{P(s'=s_t | s=s_{t-1}, E_t=l) P(E_t=l | E_{t-1}=m)}{P(s'=s_t | s_{0 \rightarrow (t-1)})}$ belongs to a set of auxiliary variables $\Gamma = [\gamma_{lh}]_{2 \times 2}$ that are calculated by the last estimate $\hat{\Theta}^{t-1}$ of the model parameters:

$$\gamma_{lh}^t = \frac{\hat{P}_{lh}^{t-1} \hat{T}_{hs_{t-1}s_t}^{t-1}}{\sum_{m,n} \hat{q}_m^{t-1} \hat{P}_{mn}^{t-1} \hat{T}_{n s_{t-1} s_t}^{t-1}}. \quad (28)$$

Then, using these auxiliary variables γ_{lh} , a set $\Phi = [\hat{\phi}_{i,j,s,s',h}]_{2 \times 2 \times 16 \times 16 \times 2}$ of parameters is recursively updated:

$$\hat{\phi}_{i,j,s,s',h}^t = \sum_l \gamma_{lh}^t \left[(1 - \eta) \hat{\phi}_{i,j,s,s',l}^{t-1} + \eta \hat{q}_l^{t-1} \Delta_{ijss'}^{lh s_{t-1} s_t} \right], \quad (29)$$

where $\Delta_{ijss'}^{lh s_{t-1} s_t} = \delta(i-l) \delta(j-h) \delta(s-s_{t-1}) \delta(s'-s_t)$, $\delta(\cdot)$ is the Kronecker delta (i.e., 1 when its argument is zero and 0 otherwise), and η is the learning rate.

Finally, the model parameters are updated by

$$\hat{P}_{ij}^t = \frac{\sum_{s,s',h} \hat{\phi}_{ijss'h}^t}{\sum_{j,s,s',h} \hat{\phi}_{ijss'h}^t}; \quad \hat{T}_{jss'}^t = \frac{\sum_{i,h} \hat{\phi}_{ijss'h}^t}{\sum_{i,s',h} \hat{\phi}_{ijss'h}^t}. \quad (30)$$

We emphasize that in order for the online EM algorithm to work properly, some technical considerations must be respected. For instance, in the beginning of learning, only online estimation of Φ must be updated (without updating the model parameters Θ), so that the estimation error for the first 2000 time steps of our simulation in Fig. 6-A (blue) remains fixed.

Appendix H: The raw surprise increases with the information content as well as with the Bayesian surprise.

The Bayesian surprise (21, 29) measures change in belief and is defined as a KL divergence $D_{KL}[\pi_0||\pi_1]$ between the prior belief π_0 and the posterior belief $\pi_0(\theta)$ that is calculated by the naive Bayes rule

$$\pi_1(\theta) = \frac{p(X|\theta)\pi_0(\theta)}{\int_{\Theta} p(X|\theta)\pi_0(\theta) d\theta}. \quad (31)$$

The raw surprise $S_{raw}(X; \pi_0)$ (1) implicitly incorporates Bayesian surprise. This is because the raw surprise can be written as two terms as following

$$\begin{aligned} S_{raw}(X; \pi_0) &\stackrel{(1)}{=} - \int_{\Theta} \pi_0(\theta) \ln p(X|\theta) d\theta \\ &\stackrel{(31)}{=} - \int_{\Theta} \pi_0(\theta) \ln \left[\frac{\pi_1(\theta) \left(\int_{\Theta} p(X|\theta)\pi_0(\theta) d\theta \right)}{\pi_0(\theta)} \right] d\theta \\ &= D_{KL}[\pi_0||\pi_1] - \ln \left[\int_{\Theta} p(X|\theta)\pi_0(\theta) d\theta \right], \end{aligned} \quad (32)$$

where the first term $D_{KL}[\pi_0||\pi_1]$ stands for the Bayesian surprise. The second term, $-\ln \int_{\Theta} p(X|\theta)\pi_0(\theta)d\theta$, is an upper bound of the information content $-\ln p(X|\theta^*)$ (and thus increases with the information content). Therefore, the raw surprise $S_{raw}(X; \pi_0)$ (32) combines both the data-driven (information content) approach of Shannon and the model-driven (Bayesian surprise) approach for measuring surprise. Note that our proposed confidence-corrected surprise measure $S_{corr}(X; \pi_0)$ (3) inherits the property of the raw surprise $S_{raw}(X; \pi_0)$ (32). As such, it also combines the benefits of both data-driven and model-driven approaches for measuring surprise.